

Second-order effective renormalized Hamiltonian of Quantum Chromodynamics

Kamil Serafin, Carter M. Gustin, and Peter J. Love*

Department of Physics and Astronomy,

Tufts University, Medford, Massachusetts 02155, USA

arXiv:2606.24699v1 [hep-ph] 23 Jun 2026

Abstract

The effective Hamiltonian of quantum chromodynamics in the front form of Hamiltonian dynamics is calculated and renormalized. The renormalization group procedure for effective particles up to the second order in the coupling constant is used. Small gluon mass is used to regulate infrared singularities of the theory. The counterterms necessary to renormalize the theory are determined by computing matrix elements of the effective Hamiltonian. The effective Hamiltonians are well-defined symmetric forms on a dense subspace of the Fock space. The zero modes are cut off but, once ultraviolet renormalization is performed, no divergences are found in the color singlet subspace in the limit of the gluon mass approaching zero. A major result is that the interplay between self-energy terms and gluon exchange effective terms generates a term proportional to the quadratic SU(3) Casimir operator times the logarithm of the gluon mass. Therefore, the matrix elements are logarithmically divergent in the color nonsinglet subspace, but finite in the color singlet subspace, because the Casimir operator vanishes in the color singlet subspace. The effective Hamiltonians are suitable for nonperturbative numerical calculations using either classical or quantum computers.

I. INTRODUCTION

In this paper we compute the effective renormalized Hamiltonian of QCD up to the second order in the expansion in the renormalized coupling constant g . This Hamiltonian represents the minimal starting point for a program of nonperturbative studies of QCD. The main ingredients of the program include the front form (FF) of Hamiltonian dynamics [1, 2], and the renormalization group procedure for effective particles (RGPEP) [3, 4].

The standard framework for nonperturbative QCD calculations is lattice QCD, in which field correlation functions are estimated on lattices of points in Euclidean space using Monte Carlo sampling methods. Lattice QCD is most successful with computations of static properties of QCD bound states, such as masses of hadrons, their magnetic moments, and decay constants. Scattering properties, such as structure functions in deep inelastic scattering, are difficult to obtain. Other calculations face fundamental difficulties due to the sign problem, which prohibits sampling methods.

* Also at Brookhaven National Laboratory

In the FF of Hamiltonian dynamics the state of the field is determined on a three-dimensional hyperplane tangent to a light cone in Minkowski spacetime. One of the characteristic properties of the FF is that the center of mass motion of a system of particles decouples from the relative motion of these particles. This means that the relative-motion wave functions of, e.g., quarks in a proton do not depend on the momentum of the proton as a whole, which makes our program particularly well-suited for relativistic scattering calculations. Paired with the FF is the choice of the light cone gauge which decouples ghosts and one deals only with physical degrees of freedom.

The RGPEP is a Wilsonian type of renormalization group in which one defines a family of effective theories expressed in terms of effective particles that interact nonlocally. The family is parameterized by a parameter $t \geq 0$ and it interpolates between bare theory with point-like particles interacting locally at $t = 0$ and the diagonal Hamiltonian at $t = \infty$. In this sense, increasing t brings the theory closer to being solved.

An additional motivation for developing the QCD program described in this article is provided by the emerging quantum computing technologies. Quantum simulation calculations are done most straightforwardly using Hamiltonian approaches, hence, FF Hamiltonians can be applied directly. Quantum computers are expected to provide new opportunities for the problems that are most difficult for lattice QCD to solve, including structure problems of bound states, real-time simulation of dynamics, and simulation of strongly correlated matter at high density or far from equilibrium. The triviality of the FF vacuum also distinguishes our approach from other proposals such as Ref. [5–7].

In perturbation theory our approach is in principle equivalent to the standard approaches. The RGPEP Hamiltonian is obtained from the bare FF Hamiltonian by means of a unitary transformation. Thus, calculations for the same quantity will yield the same result as long as the unitary transformation is calculated to the same order to which the quantity of interest is calculated. This independence of parameter t has been verified explicitly in a relativistic model based on Yukawa theory for scattering T matrix up to the fourth order in perturbation theory [8, 9]. Equivalence of the S matrix for effective and bare particles has been studied in scalar field theory, see Ref. [10].

The FF coordinates cannot be related to any inertial frame via a Lorentz transformation, hence, the FF is a substantially distinct framework. Nevertheless one can compute correlation functions of fields using perturbation theory equally well in both the standard instant

form and the FF using various techniques, such as Feynman diagrams, or old-fashioned perturbation theory. Although the final results are the same, the intermediate steps are done differently, and special attention needs to be given to the so-called zero mode contributions, whose proper inclusion can be tricky [11–14]. The physical picture of certain phenomena can also differ substantially between different forms of dynamics. The most significant difference in QCD is the role that the vacuum plays in the appearance of confinement and chiral symmetry breaking. In the instant form, both confinement and chiral symmetry breaking are directly linked to the complicated structure of the vacuum via quark and gluon condensates. In the front form all complexities of the vacuum state have to be contained in the special subset of field modes that have exactly zero longitudinal momentum—these excitations are called zero modes. Furthermore, one can remove the zero modes from the theory, but restore all of their effects on the theory by including appropriate counterterms in the Hamiltonian (and possibly other operators of interest). Therefore, a complicated vacuum in the instant form is replaced with a trivial vacuum and special counterterms in the Hamiltonian in the front form. In the field theory of a scalar field the effects of zero modes amount to unobservable shifts of bare masses and coupling constants. To the best of our knowledge, the zero-mode counterterms in QCD, whose inclusion is necessitated by the removal of the zero modes, are not fully known. One way of studying these problems is the discretized light-cone quantization (DLCQ), in which the theory is quantized in a box. Numerical solutions for 1+1D QCD done using DLCQ provide in fact a complete solution of the theory [15, 16]. Analogous calculations in 1+3-dimensional QCD are much more demanding in terms of computational resources needed to produce high-quality results. However, if given enough resources, the approach might be equally successful in 1+3D as it was in 1+1D. The multitude of results, and the continued progress done by the BLFQ Collaboration supports this claim by example [17]. While the main goal of the BLFQ Collaboration at the moment is the study of the bare canonical Hamiltonian of QCD, we provide an effective, i.e., renormalized Hamiltonian that can be studied using similar methods. Our Hamiltonian is a minimal, well-defined starting point for nonperturbative calculations in QCD. To study the influence of the missing zero-mode counterterms one might perhaps need to use methods similar to those described in Ref. [18]. In any case, numerical calculations are supposed to guide the development of the theory of the front-form zero-mode counterterms. Therefore, we make calculations in a way that should aid subsequent studies of all the important properties of

front-form Hamiltonians, including confinement, chiral symmetry breaking, and renormalizability.

References [19, 20] represent an early work on FF QCD and important applications to exclusive processes were investigated in Ref. [21]. Various problems of the canonical FF QCD Hamiltonian have been studied in Refs. [22–24], including coupling constant renormalization and asymptotic freedom [24, 25]. Recent numerical studies within the framework of basis light-front quantization (BLFQ) [26, 27] use Fock-sector-dependent renormalization [28–30]. Other authors emphasize regulators that preserve Lorentz and gauge symmetries at the expense of introducing Pauli-Villars ghost fields [31, 32]. Chiral symmetry and constrained fermion zero modes in QCD that induce effective interactions were studied in, e.g., Ref. [33].

Investigations of the QCD Hamiltonian using the similarity renormalization group (SRG) [34, 35] begin with Ref. [36]. Important findings following the approach of [36] include cancellation of infrared divergences and the presence of logarithmic confining potentials within the color-singlet Fock subspace [37]. These potentials rise twice as quickly in the transverse direction as they do in the longitudinal direction. In contrast, in 1+2-dimensional QCD the analogous potentials are linear in the transverse direction, while of the square root form in the longitudinal direction [38]. Bound state studies of heavy-light mesons and heavy quarkonia using early versions of SRG have been pursued [39, 40]. Following the principle of coupling coherence [41, 42], Yang-Mills Hamiltonian, and spectra and wave functions of glueballs have been found [43]. Within heavy-flavor QCD an approach based on the gluon mass ansatz has been proposed [44]. In principle, infinitely many Fock sectors can be integrated out. The ansatz is that gluons in the remaining sectors acquire an effective mass which crudely represents effects of nonperturbative partial diagonalization necessary to reduce the Hamiltonian. This approach has been applied to heavy quarkonia [45, 46], triply heavy baryons [47], as well as glueballs [48]. For separations between heavy quarks typical for the ground states of heavy quarkonia, the confining potentials are approximately harmonic and rotationally symmetric as opposed to the long-distance logarithmic behavior [49]. Using a form of the RGPEP closely resembling our calculations, asymptotic freedom has been confirmed in a calculation of the effective triple-gluon vertex [50].

In a previous article, Ref. [51], we computed the second-order effective Hamiltonian of Yukawa theory and we introduced a technique based on Wick’s diagrams in momentum space. Wick’s diagrams are meant to formalize a graphical representation of the mathemat-

ical formulas for interaction operators in the effective Hamiltonian. Importantly, a single diagram typically represents several distinct time orderings, e.g., gluon splitting into two gluons and two gluons merging into a single gluon are represented with one triple-gluon Wick’s diagram. This method has been developed to the extent necessary at the second order of perturbation theory for the effective Hamiltonians.

In this article we use methods developed in Ref. [51] to compute the full expression for the second-order effective Hamiltonian of QCD on the light-front, thereby extending the results of Ref. [49] to all Fock sectors. We start with the canonical FF Hamiltonian of QCD and remove zero modes from interactions with longitudinal momentum cutoff $p^+ > \epsilon^+$. This ensures triviality of the vacuum but requires inclusion of zero-mode counterterms that will fully reproduce effects of confinement and chiral symmetry breaking—a task that we postpone to a later work. The zero-mode counterterms may shift bare masses and coupling constants. Therefore, at least part of the zero-mode counterterms can be recovered by simply fitting the unperturbed masses, and the coupling constant to reproduce a small set of observables (a step that is reasonable in any case). Analogous shifts in the scalar theory, in fact, include all effects of the removed zero modes [52, 53]. In the same vein, since chiral symmetry breaking leads to quarks acquiring large effective masses, allowing large values for quark masses in the fitting process will make it possible to reproduce at least some effects of chiral symmetry breaking.

Following Ref. [49], we also introduce a gluon mass, m_g to regulate the singularities that arise when longitudinal momentum of a gluon approaches zero. This regulator likely breaks gauge invariance of correlation functions computed perturbatively using the effective Hamiltonians. Therefore, having renormalized the ultraviolet divergences in the Hamiltonian, we perform the $m_g \rightarrow 0$ limit, which will restore the standard results (to the extent that the canonical Hamiltonian without zero-mode counterterms can produce). Gauge symmetry is not manifest in our approach from the very start, since we fix the gauge to the light-cone gauge. The main purpose of the effective Hamiltonians that we compute is to use them in nonperturbative calculations using, e.g., DLCQ or BLFQ. For that purpose, breaking of gauge and Lorentz symmetry is acceptable [36]. In fact, the choice of the RGPEP generator that we make further breaks the exact longitudinal boost invariance of the FF. This is due to the approximate nature of the solutions of the RGPEP equations that we compute. If we could solve these equations exactly, the longitudinal boost invariance would also be exact.

Despite the omission of the zero-mode counterterms removal of the infrared regularization in the renormalized effective Hamiltonian, i.e., the $m_g \rightarrow 0$ limit, yields a well-defined theory in the color-singlet Fock subspace. This is because all terms that depend on the gluon mass are proportional to a Casimir operator of $SU(3)$, which vanishes in the singlet sector. This is in apparent contradiction with Refs. [22, 36]. Additionally, as opposed to Ref. [36], we do not include any universally confining potential, whose inclusion in Ref. [36] was motivated by a potential instability of the Hamiltonian. At this point there appears no need for such measures. Numerical simulations should detect the instability, should it be present in our Hamiltonians.

The paper is organized as follows. The canonical Hamiltonian of QCD is reviewed and notation is established in Sec. II. In Sec. III we discuss the regulating factors that we introduce. The effective Hamiltonian is computed up to the second order in Sec. IV. In Sec. V we study the matrix elements of the effective Hamiltonian and determine the counterterms that need to be added to the bare Hamiltonian to make the effective Hamiltonian well defined in the limit of removing the ultraviolet regularization. Section VI concerns the limit of removing the infrared regulating gluon mass and the quadratic Casimir operator is found. Section VII summarizes the effective Hamiltonian, and we make concluding remarks in Sec. VIII.

II. CANONICAL HAMILTONIAN OF QCD

The canonical Hamiltonian is the integral of the density over the hypersurface defined by $x^+ = 0$,

$$H_{\text{canonical}} = \int dx^- d^2x^\perp \mathcal{H} . \quad (1)$$

The density of the canonical Hamiltonian of QCD in the Front Form of Hamiltonian dynamics is,

$$\mathcal{H} = \mathcal{H}_{\psi^2+A^2} + \mathcal{H}_{jA} + \mathcal{H}_{A^4} + \mathcal{H}_{\psi AA\psi} + \mathcal{H}_{jj} , \quad (2)$$

where

$$\mathcal{H}_{\psi^2+A^2} = \mathcal{N} \left(\bar{\psi} \frac{\gamma^+ (i\partial^\perp)^2 + m^2}{i\partial^+} \psi \right) + \mathcal{N} \left\{ \frac{1}{2} A^{ia} [m_g^2 + (i\partial^\perp)^2] A^{ia} \right\}, \quad (3)$$

$$\mathcal{H}_{j_A} = j_{q\mu}^a A^{\mu a} + j_{g\mu}^a A^{\mu a}, \quad (4)$$

$$\mathcal{H}_{A^4} = \frac{1}{4} g^2 f^{abc} f^{ade} \mathcal{N} (A_\alpha^b A_\beta^c A^{\alpha d} A^{\beta e}), \quad (5)$$

$$\mathcal{H}_{\psi AA\psi} = \frac{1}{2} g^2 \mathcal{N} \left(\bar{\psi} \gamma^i A^{ia} T^a \frac{\gamma^+}{i\partial^+} \gamma^j A^{jb} T^b \psi \right), \quad (6)$$

$$\mathcal{H}_{jj} = \frac{1}{2} \mathcal{N} \left[(j_q^{+a} + 3j_g^{+a}) \frac{1}{(i\partial^+)^2} (j_q^{+a} + 3j_g^{+a}) \right], \quad (7)$$

ψ is the quark field and A is the gluon field, and $j_q^{\mu a}$ and $j_g^{\mu a}$ are hermitian color current operators,

$$j_q^{\mu a} = g \mathcal{N} (\bar{\psi} \gamma^\mu T^a \psi), \quad (8)$$

$$\begin{aligned} j_g^{\mu c} = & g^{\mu\gamma} \frac{g}{3!} i f^{abc} \{ g_{\alpha\beta} [A^{\alpha a}(x) i\partial_\gamma A^{\beta b}(x) - i\partial_\gamma A^{\alpha a}(x) A^{\beta b}(x)] \\ & - g_{\beta\gamma} [i\partial_\alpha A^{\alpha a}(x) A^{\beta b}(x) + 2A^{\alpha a}(x) i\partial_\alpha A^{\beta b}(x)] \\ & + g_{\gamma\alpha} [2i\partial_\beta A^{\alpha a}(x) A^{\beta b}(x) + A^{\alpha a}(x) i\partial_\beta A^{\beta b}(x)] \}. \end{aligned} \quad (9)$$

Indices $a, b, c, d, e = 1, \dots, 8$ denote color. Indices $i, j = 1, 2$ denote the components of the transverse momentum two-vectors.

The definition, Eq. (9) differs from other, notable definitions used before. For example, for the purpose of defining the canonical Hamiltonian one could use a nonsymmetric gluon color current of the form $j_{\text{NS}}^{\mu a} = -ig f^{abc} A^{jb} i\partial^\mu A^{jc}$, which is the same as the gluon color current $\tilde{\chi}^{\mu a}$ defined in Ref. [1], see Eq. (2.79) there. The Hamiltonian density, \mathcal{H} , as defined above with the use of $j_g^{\mu a}$, is the same as that given in Ref. [1], where $\tilde{\chi}^{\mu a}$ was used. Since, $j_{\text{NS}}^{+a} = 3j_g^{+a}$, using $j_{\text{NS}}^{\mu a}$ is convenient when writing down instantaneous Hamiltonian term \mathcal{H}_{jj} , because there would be no need for the factors of 3 in Eq. (7). Our choice leads more directly to the symmetric form of the three-gluon vertex in momentum space, see Eq. (31). This choice also fits better the structure of later calculations, in which two three-gluon vertices are contracted with each other, and a symmetry factor needs to be included because contractions of different legs of the two vertices leads to the same Hamiltonian terms. In this sense, the canonical instantaneous-gluon interaction \mathcal{H}_{jj} is interpreted as composed of two three-leg diagrams. If either of the diagrams is a three-gluon vertex, then there is a three-fold choice of which of the gluon legs is to be contracted.¹ Therefore, calculations in

¹ $j_{g\mu}^a A^{\mu a}$ is not a contraction of two diagrams, and does not require any symmetry factors.

which symmetric three-gluon vertices are used, and in which the instantaneous vertices can be interpreted as contractions of two three-leg interactions, seem more consistent. Although in the second-order calculations we already see the utility of our choice, we anticipate that the effort of keeping track of all the factors of 3 will be most useful in calculations of order higher than the second.

The quark field is assigned mass m , while the gluon field is assigned mass m_g . The gluon mass is an important modification of the usual QCD Hamiltonian introduced to regulate singularities associated with the vanishing longitudinal momentum of gluons. The fields are expanded in the plane wave basis,

$$\psi(x) = \sum_{c,\sigma} \int \frac{dp^+ d^2 p^\perp}{16\pi^3 p^+} \theta(p^+) [\chi_c u_\sigma(p) e^{-ipx} b_{p\sigma c} + \chi_c v_\sigma(p) e^{ipx} d_{p\sigma c}^\dagger], \quad (10)$$

$$A^{\mu c}(x) = \sum_\sigma \int \frac{dp^+ d^2 p^\perp}{16\pi^3 p^+} \theta(p^+) [\varepsilon_\sigma^\mu(p) e^{-ipx} a_{p\sigma c} + \varepsilon_\sigma^{\mu*}(p) e^{ipx} a_{p\sigma c}^\dagger], \quad (11)$$

where $b_{p\sigma c}$, and $d_{p\sigma c}$ are annihilation operators for a quark and an antiquark with momentum p , light-front helicity, i.e., spin projection onto z axis, $\sigma = \pm\frac{1}{2}$, and color $c = 1, 2, 3$, respectively. Gluon with momentum p , light-front helicity $\sigma = \pm 1$, and color $c = 1, \dots, 8$ is annihilated with an operator $a_{p\sigma c}$. With quarks and antiquarks are associated spinors $u_\sigma(p)$ and $v_\sigma(p)$, which are solutions of the free Dirac equation, and the color three-vector $\chi_c = [\delta_{c,1}, \delta_{c,2}, \delta_{c,3}]^T$, where T denotes transposition. Gluons have a polarization four-vector $\varepsilon_\sigma^\mu(p)$ associated with them, and the star in $\varepsilon_\sigma^{\mu*}(p)$ means complex conjugation. $\varepsilon_\sigma^+(p) = 0$ and $p_\mu \varepsilon_\sigma^\mu(p) = 0$. Since the longitudinal component of the angular momentum is conserved exactly in the front form, circular polarization vectors, e.g., $\varepsilon_{\pm 1}^\perp = [\mp 1, -i]^T / \sqrt{2}$, are a useful choice.

We define the Fourier transforms, $\Psi(q)$, $G^{\mu a}(q)$, $J_q^{\mu a}(q)$, and $J_g^{\mu a}(q)$ of $\psi(x)$, $A^{\mu a}(x)$, $j_q^{\mu a}(q)$, and $j_g^{\mu a}(q)$, respectively, in accordance with the generic formula,

$$F(q) = \int dx^- d^2 x^\perp e^{\frac{i}{2} q^+ x^- - i q^\perp x^\perp} f(x). \quad (12)$$

Thus,

$$\Psi(q) = \sum_{c,\sigma} \frac{\theta(q^+) \chi_c u_\sigma(q) b_{q\sigma c} + \theta(-q^+) \chi_c v_\sigma(-q) d_{-q\sigma c}^\dagger}{|q^+|}, \quad (13)$$

$$G^{\mu a}(q) = \sum_{\sigma} \frac{\theta(q^+) \varepsilon_{\sigma}^{\mu}(q) a_{q\sigma c} + \theta(-q^+) \varepsilon_{\sigma}^{\mu*}(-q) a_{-q\sigma c}^\dagger}{|q^+|}, \quad (14)$$

$$J_{q/g}^{\mu a}(q) = \int [q_1 q_2] \tilde{\delta}_{12,q} \tilde{J}_{q/g}^{\mu a}(q_1, q_2), \quad (15)$$

where

$$\tilde{J}_q^{\mu a}(q_1, q_2) = g \mathcal{N} [\bar{\Psi}(-q_1) \gamma^\mu T^a \Psi(q_2)], \quad (16)$$

$$\tilde{J}_g^{\mu c}(q_1, q_2) = g^{\mu\gamma} \frac{g}{3!} F_{\alpha\beta\gamma}^{abc}(q_1, q_2, -q_1 - q_2) G^{\alpha a}(q_1) G^{\beta b}(q_2), \quad (17)$$

and

$$F_{\alpha\beta\gamma}^{abc}(q_1, q_2, q_3) = i f^{abc} [(q_{2\gamma} - q_{1\gamma}) g_{\alpha\beta} + (q_{3\alpha} - q_{2\alpha}) g_{\beta\gamma} + (q_{1\beta} - q_{3\beta}) g_{\gamma\alpha}]. \quad (18)$$

$F_{\alpha\beta\gamma}^{abc}(q_1, q_2, q_3)$ differs from the usual three-gluon vertex factor used in Feynman diagrams only by a constant factor. The current densities satisfy

$$\tilde{J}_{q/g}^{\mu c}(q_1, q_2)^\dagger = \tilde{J}_{q/g}^{\mu c}(-q_2, -q_1), \quad (19)$$

$$\tilde{J}_g^{\mu c}(q_2, q_1) = \tilde{J}_g^{\mu c}(q_1, q_2), \quad (20)$$

$$(q_{1\mu} + q_{2\mu}) \tilde{J}_{q/g}^{\mu c}(q_1, q_2) = 0, \quad (21)$$

$$q_\mu \tilde{J}_{q/g}^{\mu c}(q_1, q_2) = \frac{q^- - q_1^- - q_2^-}{2} \tilde{J}_{q/g}^{+c}(q_1, q_2), \quad (22)$$

with $q^{+,\perp} = q_1^{+,\perp} + q_2^{+,\perp}$, but $q^- \neq q_1^- + q_2^-$ in general, i.e., $q^\mu = q_1^\mu + q_2^\mu + n^\mu (q^- - q_1^- - q_2^-)/2$, where n^μ is a null fourvector tangent to the light front hypersurface such that $n^- = 2$, and $n^+ = n^1 = n^2 = 0$, while the nonzero elements of the metric tensor are $g^{+-} = g^{-+} = 2$, $g^{11} = g^{22} = -1$. To prove Eq. (22) for quark current density Dirac equation, $\not{q}\Psi(q) = m\Psi(q)$ is used, while for gluon current density $q_\mu G^{\mu c}(q) = 0$, and $q_{1\mu} q_1^\mu = q_{2\mu} q_2^\mu$ are used.

Note that q^+ can be both positive and negative and the Fourier transform is three-dimensional, hence, Ψ and G are functions of q^+ and q^\perp only. One can, however, assign q^- components in accordance to free evolution,

$$i\partial_f^- \Psi(q) = q^- \Big|_m \Psi(q), \quad (23)$$

$$i\partial_f^- \bar{\Psi}(-q) = q^- \Big|_m \bar{\Psi}(-q), \quad (24)$$

$$i\partial_f^- G(q) = q^- \Big|_{m_g} G(q), \quad (25)$$

where $q^-|_m = \frac{m^2+(q^\perp)^2}{q^+}$, $q^-|_{m_g} = \frac{m_g^2+(q^\perp)^2}{q^+}$.

The canonical Hamiltonian is,

$$H_{\text{canonical}} = H_{\psi^2+G^2} + H_{\psi^2G} + H_{G^3} + \mathcal{H}_{G^4} + H_{\psi^2G^2} + H_{JJ} . \quad (26)$$

It consists of the free part, and first- and second-order vertices. For illustration purposes we represent interaction terms as Wick's diagrams [51]. We also introduce simplified notation:

$$\tilde{\delta}_{1\dots n} = 16\pi^3 \delta(q_1^+ + \dots + q_n^+) \delta^2(q_1^\perp + \dots + q_n^\perp) , \quad (27)$$

$$[q] = \frac{dq^+ d^2q^\perp}{16\pi^3} , \quad [q_1 q_2] = [q_1][q_2] , \quad \text{etc.} \quad (28)$$

The free part of the Hamiltonian is,

$$H_{\psi^2+G^2} = \int [q] q^-|_m \mathcal{N} \left[\bar{\Psi}(q) \frac{\gamma^+}{2} \Psi(q) \right] + \int [q] q^+ q^-|_{m_g} \mathcal{N} \left[\frac{1}{2} G^{ia}(-q) G^{ia}(q) \right] . \quad (29)$$

There are two first-order vertices. The quark-gluon vertex is,

$$H_{\psi^2G} = g \int [q_1 q_2 q_3] \tilde{\delta}_{123} \mathcal{N} \left[\bar{\Psi}(-q_1) \gamma_\mu T^a \Psi(q_2) G^{\mu a}(q_3) \right] , \quad (30)$$

and it is represented in Fig. 1(a). The triple gluon vertex is,

$$H_{G^3} = \frac{g}{3!} \int [q_1 q_2 q_3] \tilde{\delta}_{123} F_{\alpha\beta\gamma}^{abc}(q_1, q_2, q_3) G^{\alpha a}(q_1) G^{\beta b}(q_2) G^{\gamma c}(q_3) . \quad (31)$$

It is represented as a Wick's diagram in Fig. 1(b).

There are three second-order vertices. The first one is the usual four-gluon vertex,

$$H_{G^4} = \frac{g^2}{4!} \int [q_1 q_2 q_3 q_4] \tilde{\delta}_{1234} F_{\alpha\beta\gamma\delta}^{abcd} \mathcal{N} \left[G^{\alpha a}(q_1) G^{\beta b}(q_2) G^{\gamma c}(q_3) G^{\delta d}(q_4) \right] , \quad (32)$$

where

$$F_{\alpha\beta\gamma\delta}^{abcd} = f^{abe} f^{cde} (g_{\alpha\gamma} g_{\beta\delta} - g_{\alpha\delta} g_{\beta\gamma}) + f^{ace} f^{bde} (g_{\alpha\beta} g_{\gamma\delta} - g_{\alpha\delta} g_{\beta\gamma}) + f^{ade} f^{bce} (g_{\alpha\beta} g_{\gamma\delta} - g_{\alpha\gamma} g_{\beta\delta}) . \quad (33)$$

The four-gluon vertex is symmetrized from its nonsymmetric form of Eq. (5). This interaction term is represented as a Wick's diagram in Fig. 1(c). The other two second-order vertices are characteristic to the front form and are called instantaneous. The instantaneous fermion vertex is,

$$H_{\psi^2G^2} = \frac{1}{2} g^2 \int [q_1 q_2 q_3 q_4] \tilde{\delta}_{1234} \mathcal{N} \left[\bar{\Psi}(-q_1) \gamma^i G^{ia}(q_2) T^a \frac{\gamma^+}{q_3^+ + q_4^+} \gamma^j G^{jb}(q_3) T^b \Psi(q_4) \right] . \quad (34)$$

It is represented as a Wick's diagram in Fig. 2(a). The instantaneous gluon interaction is,

$$H_{JJ} = \frac{1}{2} \int [q] \mathcal{N} \left\{ \left[J_q^{+a}(-q) + 3J_g^{+a}(-q) \right] \frac{1}{(q^+)^2} \left[J_q^{+a}(q) + 3J_g^{+a}(q) \right] \right\} . \quad (35)$$

This vertex has four contributions represented as Wick's diagrams in Fig. 2(b)–(e).

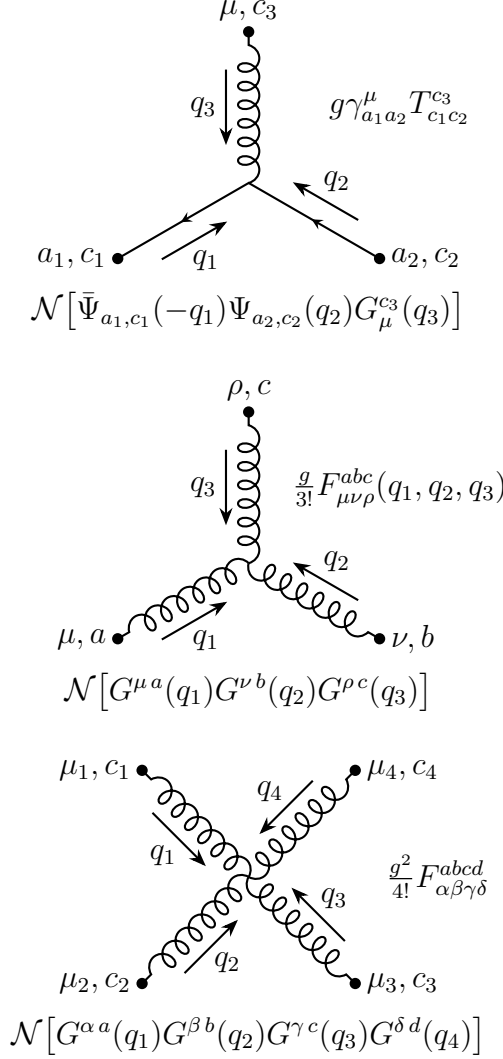


FIG. 1. Basic diagrams.

III. REGULARIZED HAMILTONIAN OF QCD

The first cutoff we introduce is the small p^+ cutoff in the Fourier expansion of fields,

$$\psi(x) = \sum_{c, \sigma} \int \frac{dp^+ d^2 p^\perp}{16\pi^3 p^+} \theta_\epsilon(p^+) [\chi_c u_\sigma(p) e^{-ipx} b_{p\sigma c} + \chi_c v_\sigma(p) e^{ipx} d_{p\sigma c}^\dagger], \quad (36)$$

$$A^{\mu c}(x) = \sum_{\sigma} \int \frac{dp^+ d^2 p^\perp}{16\pi^3 p^+} \theta_\epsilon(p^+) [\varepsilon_{\sigma}^{\mu}(p) e^{-ipx} a_{p\sigma c} + \varepsilon_{\sigma}^{\mu*}(p) e^{ipx} a_{p\sigma c}^\dagger], \quad (37)$$

where $\theta_\epsilon(p^+) = \theta(p^+ - \epsilon^+)$, and $\epsilon^+ > 0$ is the minimal p^+ any mode can have. Therefore,

$$\Psi(q) = \sum_{c, \sigma} \frac{\theta_\epsilon(q^+) u_\sigma(q) b_{q\sigma c} + \theta_\epsilon(-q^+) v_\sigma(-q) d_{-q\sigma c}^\dagger}{|q^+|} \chi_c, \quad (38)$$

$$G^{\mu c}(q) = \sum_{\sigma} \frac{\theta_\epsilon(q^+) \varepsilon_{\sigma}^{\mu}(q) a_{q\sigma c} + \theta_\epsilon(-q^+) \varepsilon_{\sigma}^{\mu*}(-q) a_{-q\sigma c}^\dagger}{|q^+|}. \quad (39)$$

$$\mathcal{N} \left[\bar{\Psi}_{a_1, c_1}(-q_1) \Psi_{a_2, c_2}(q_2) G^{\mu c_3}(q_3) G^{\nu c_4}(q_4) \right]$$

$$\frac{g^2}{2q_5^+} [\gamma_\mu \gamma^+ \gamma_\nu]_{a_1 a_2} T_{c_1, c_5}^{c_3} T_{c_5, c_2}^{c_4}$$

$$\mathcal{N} \left[\bar{\Psi}_{a_1, c_1}(-q_1) \Psi_{a_2, c_2}(q_2) \bar{\Psi}_{a_3, c_3}(-q_3) \Psi_{a_4, c_4}(q_4) \right]$$

$$\frac{g^2}{2q_5^+} [\gamma^+]_{a_1 a_2} [\gamma^+]_{a_3 a_4} T_{c_1, c_2}^{c_5} T_{c_3, c_4}^{c_5}$$

$$\mathcal{N} \left[\bar{\Psi}_{a_1, c_1}(-q_1) \Psi_{a_2, c_2}(q_2) G^{\mu c_3}(q_3) G^{\nu c_4}(q_4) \right]$$

$$\frac{g^2}{2q_5^+} [\gamma^+]_{a_1 a_2} \frac{q_3^+ - q_4^+}{2} g_{\mu\nu} T_{c_1, c_2}^{c_5} i f^{c_5 c_3 c_4}$$

$$\mathcal{N} \left[G^{\mu_1 c_1}(q_1) G^{\mu_2 c_2}(q_2) G^{\mu_3 c_3}(q_3) G^{\mu_4 c_4}(q_4) \right]$$

$$\frac{g^2}{2q_5^+} \frac{q_1^+ - q_2^+}{2} g_{\mu_1 \mu_2} \frac{q_3^+ - q_4^+}{2} g_{\mu_3 \mu_4} i f^{c_5 c_1 c_2} i f^{c_5 c_3 c_4}$$

$$\mathcal{N} \left[G^{\mu c_1}(q_1) G^{\nu c_2}(q_2) \bar{\Psi}_{a_3, c_3}(-q_3) \Psi_{a_4, c_4}(q_4) \right]$$

$$\frac{g^2}{2q_5^+} \frac{q_1^+ - q_2^+}{2} g_{\mu\nu} [\gamma^+]_{a_3 a_4} i f^{c_5 c_1 c_2} T_{c_3, c_4}^{c_5}$$

FIG. 2. Instantaneous diagrams.

The purpose of this cutoff is to remove interactions that would produce zero modes from the vacuum, thus ensuring the triviality of the vacuum state. The limit $\epsilon^+ \rightarrow 0^+$ is the first limit to be taken.

Local interactions in QCD lead to ultraviolet divergences, which make the canonical Hamiltonian not well defined. Hence, we redefine the interaction terms of the canonical Hamiltonian. The three-leg interactions become,

$$H_{\psi^2 G} = g \int [q_1 q_2 q_3] f_{t_r, 123}^q \tilde{\delta}_{123} \mathcal{N} \left[\bar{\Psi}(-q_1) \gamma_\mu T^a \Psi(q_2) G^{\mu a}(q_3) \right], \quad (40)$$

$$H_{G^3} = \frac{g}{3!} \int [q_1 q_2 q_3] f_{t_r, 123}^g \tilde{\delta}_{123} F_{\alpha\beta\gamma}^{abc}(q_1, q_2, q_3) G^{\alpha a}(q_1) G^{\beta b}(q_2) G^{\gamma c}(q_3), \quad (41)$$

where t_r is the cutoff parameter, and $f_{t_r, 123}^q$ and $f_{t_r, 123}^g$ are regulating functions,

$$f_{t_r, 123}^q = \exp \left[-t_r \left(q_1^-|_m + q_2^-|_m + q_3^-|_{m_g} \right)^2 \right]. \quad (42)$$

and

$$f_{t_r,123}^g = \exp \left[-t_r \left(q_1^-|_{m_g} + q_2^-|_{m_g} + q_3^-|_{m_g} \right)^2 \right]. \quad (43)$$

The subscripts in $f_{t_r,123}^q$ and $f_{t_r,123}^g$ are not to be confused as containing number 123, but rather three numbers, 1, 2, and 3 that represent momenta of particles 1, 2, and 3, respectively. Note that the order of subscripts matters. The difference between $f_{t_r,123}^q$ and $f_{t_r,123}^g$ is in the definition of the minus components of q_i s. For $f_{t_r,123}^q$, the definition of q_1^- , q_2^- , and q_3^- ensures $q_1^2 = q_2^2 = m^2$, and $q_3^2 = m_g^2$. For $f_{t_r,123}^g$, the definition of q_1^- , q_2^- , and q_3^- ensures $q_1^2 = q_2^2 = q_3^2 = m_g^2$. If one can infer from the context what the masses that need to be used for each q_i^- are, then one can drop the mass annotation of q_i^- and simply write $f_{t_r,123}$, without the superscript q or g . Note that this may lead to false simplifications, e.g., $f_{t_r,123}^q A + f_{t_r,123}^g B \neq f_{t_r,123}(A + B)$. For clarity we will keep the superscripts. The limit $t_r \rightarrow 0$ makes $f_{t_r,123}^{q/g} \rightarrow 1$, and it corresponds to the removal of the regularization.

The four-gluon vertex is redefined with a similar regulating function,

$$H_{G^4} = \frac{g^2}{4!} \int [q_1 q_2 q_3 q_4] f_{t_r,1234} \tilde{\delta}_{1234} F_{\alpha\beta\gamma\delta}^{abcd} \mathcal{N} [G^{\alpha a}(q_1) G^{\beta b}(q_2) G^{\gamma c}(q_3) G^{\delta d}(q_4)], \quad (44)$$

where

$$f_{t_r,1234} = \exp \left[-t_r \left(q_1^-|_{m_g} + q_2^-|_{m_g} + q_3^-|_{m_g} + q_4^-|_{m_g} \right)^2 \right]. \quad (45)$$

The instantaneous fermion vertex is,

$$H_{\psi^2 G^2} = \frac{1}{2} g^2 \int [q_1 q_2 q_3 q_4 q_5] \tilde{\delta}_{1234} \tilde{\delta}_{34.5} f_{t_r,1(-5)2}^q f_{t_r,(-5)43}^q \times \mathcal{N} \left[\bar{\Psi}(-q_1) \gamma^i G^{ia}(q_2) T^a \frac{\gamma^+}{q_5^+} \gamma^j G^{jb}(q_3) T^b \Psi(q_4) \right], \quad (46)$$

where

$$\tilde{\delta}_{34.5} = 16\pi^3 \delta(q_3^+ + q_4^+ - q_5^+) \delta^2(q_3^\perp + q_4^\perp - q_5^\perp), \quad (47)$$

and -5 in $f_{t_r,1(-5)2}^q$ and in $f_{t_r,(-5)43}^q$ means that q_5 momentum is to be taken with minus sign in Eq. (42). Momentum q_5 is introduced by adding one more integration and one more Dirac delta, and it serves two purposes. Firstly, q_5^+ is a place holder for $q_3^+ + q_4^+$. Secondly, q_5^- (which is not equal to $q_3^- + q_4^-$) in the regulating function $f_{t_r,1(-5)2}^q f_{t_r,(-5)43}^q$, makes the regularization act as if there were an actual particle between the two three-leg vertices depicted in Fig. 2(a).

The instantaneous gluon vertex is redefined to be,

$$H_{JJ} = \frac{1}{2} \int [q] \mathcal{N} \left\{ [J_{q,t_r}^{+a}(-q) + 3J_{g,t_r}^{+a}(-q)] \frac{1}{(q^+)^2} [J_{q,t_r}^{+a}(q) + 3J_{g,t_r}^{+a}(q)] \right\}, \quad (48)$$

where

$$J_{q/g,t_r}^{\mu a}(q) = g \int [q_1 q_2] \tilde{\delta}_{12,q} f_{t_r,12(-q)}^{q/g} \tilde{J}_{q/g}^{\mu a}(q). \quad (49)$$

q does not have a subscript, hence in $\tilde{\delta}_{12,q}$ and $f_{t_r,12(-q)}^{q/g}$ we use q itself instead of its subscript. These expressions are constructed in exactly the same way as they would be with a subscripted momentum (such as q_5 in $\tilde{\delta}_{34,5}$ and $f_{t_r,1(-5)2}^q$). The instantaneous gluon vertex is regulated as if it were composed of two three-leg vertices. This makes it consistent with the regularization functions encountered in composite terms obtained by Wick's contractions, which in terms of Wick's diagrams means connecting individual Wick's diagrams into composite ones.

Due to the gluon mass, m_g the UV regularization factors, $f_{t_r,123}^q, f_{t_r,123}^g$ regulate also what may be considered infrared singularities, i.e., factors of longitudinal momentum in the denominator, such as $1/q_5^+$ in Eq. (46) or $1/(q^+)^2$ in Eq. (48). This happens because whenever gluon momentum q^+ approaches zero, its energy $q^- = [m_g^2 + (q^\perp)^2]/q^+$ diverges making $f_{t_r,123}^{q/g}$ vanish exponentially quickly. With $m_g = 0$ it is possible to approach $q^+ = 0$ without making the gluon energy q^- diverge, for example by keeping $q^\perp = 0$ or by making q^\perp simultaneously approach 0. Since $f_{t_r,123}^q, f_{t_r,123}^g$ vanishes exponentially quickly it can regulate any fixed, negative power of q^+ . The gluon mass is treated as simply another regularization. We study the $m_g \rightarrow 0$ limit in Sec. VI.

IV. EFFECTIVE INTERACTIONS

The effective Hamiltonian, \mathcal{H}_t is defined by the following set of equations:

$$\mathcal{H}_t = H_0, \quad (50)$$

$$\frac{d}{dt} \mathcal{H}_t = [\mathcal{G}_t, \mathcal{H}_t], \quad (51)$$

where H_0 is the initial Hamiltonian with local interactions, and \mathcal{G}_t is the generator of the unitary transformation. We choose the generator in the following form,

$$\mathcal{G}_t = [\mathcal{H}_f, \mathcal{H}_t] = -i\partial_f^- \mathcal{H}_t, \quad (52)$$

where $\mathcal{H}_f = H_{\psi^2+G^2}$ is the free Hamiltonian, i.e., one obtained by putting the coupling constant, $g = 0$.

Equation (51) is a nonlinear differential equation on the space of operators, hence, exact solutions are not easy to find. For QCD one can take advantage of asymptotic freedom and compute effective Hamiltonians in perturbative expansion in powers of the coupling constant. At sufficiently high energy scales, such expansion should reproduce the exact solution well enough for the effective Hamiltonians to have eigenspectra close to the exact eigenspectrum. By defining the interacting Hamiltonian,

$$\mathcal{H}_{It} = \mathcal{H}_t - \mathcal{H}_f , \quad (53)$$

we get,

$$\frac{d}{dt}\mathcal{H}_t = -(i\partial_f^-)^2\mathcal{H}_{It} + [-i\partial_f^-\mathcal{H}_{It}, \mathcal{H}_{It}] . \quad (54)$$

where we used the fact that $\partial_f^-\mathcal{H}_f = 0$ to replace $\partial_f^-\mathcal{H}_t$ with $\partial_f^-\mathcal{H}_{It}$. Furthermore, we introduce the reduced Hamiltonian, h_t through,

$$\mathcal{H}_{It} = e^{-t(i\partial_f^-)^2} h_t . \quad (55)$$

The RGPEP equation becomes,

$$\frac{d}{dt}h_t = e^{t(i\partial_f^-)^2} [-i\partial_f^-\mathcal{H}_{It}, \mathcal{H}_{It}] . \quad (56)$$

We expand in powers of the coupling constant g ,

$$h_t = h_{t,1} + h_{t,2} + h_{t,3} + \dots , \quad (57)$$

where $h_{t,n} \sim g^n$. We arrive at a set of equations, order by order,

$$\frac{dh_{t,1}}{dt} = 0 , \quad (58)$$

$$\frac{dh_{t,2}}{dt} = e^{t(i\partial_f^-)^2} [-i\partial_f^-\mathcal{H}_{t,1}, \mathcal{H}_{t,1}] , \quad (59)$$

$$\frac{dh_{t,3}}{dt} = e^{t(i\partial_f^-)^2} [-i\partial_f^-\mathcal{H}_{t,1}, \mathcal{H}_{t,2}] + e^{t(i\partial_f^-)^2} [-i\partial_f^-\mathcal{H}_{t,2}, \mathcal{H}_{t,1}] , \quad \text{etc.}, \quad (60)$$

where $\mathcal{H}_{t,k} = e^{-t(i\partial_f^-)^2} h_{t,k}$. In the remainder, we solve these equations up to second order.

A. First order

The first-order RGPEP Eq. (58) has a simple solution,

$$h_{t,1} = h_{0,1} = H_{\psi^2 G} + H_{G^3} . \quad (61)$$

Therefore,

$$\begin{aligned} \mathcal{H}_{t,1} &= g \int [q_1 q_2 q_3] \tilde{\delta}_{123} f_{t+t_r,123}^q \mathcal{N} [\bar{\Psi}(-q_1) \gamma_\mu T^a \Psi(q_2) G^{\mu a}(q_3)] \\ &+ \frac{g}{3!} \int [q_1 q_2 q_3] \tilde{\delta}_{123} f_{t+t_r,123}^g F_{\alpha\beta\gamma}^{abc}(q_1, q_2, q_3) G^{\alpha a}(q_1) G^{\beta b}(q_2) G^{\gamma c}(q_3). \end{aligned} \quad (62)$$

The interactions acquire an effective form factor $f_{t,123}$, which is combined with the regulating factor $f_{t_r,123} f_{t,123} = f_{t+t_r,123}$. As in the case of Yukawa theory, the first order solution lowers the energy cutoff from $1/\sqrt{t_r}$ at $t = 0$ to $1/\sqrt{t+t_r}$ at $t > 0$. The matrix elements of $\mathcal{H}_{t,1}$ are insensitive to t_r in the limit $t_r \rightarrow 0^+$.

B. Second order

The second-order calculation is slightly more complicated than in Yukawa theory [51] because there are two first-order, three-leg vertices. The two copies of $\mathcal{H}_{t,1}$ in the commutator in Eq. (59) lead to four terms,

$$\frac{d}{dt} h_{t,2} = \int [q_1 q_2 q_3 q_4 q_5 q_6] \tilde{\delta}_{123} \tilde{\delta}_{456} (\mathcal{A}'_t + \mathcal{B}'_t + \mathcal{C}'_t + \mathcal{D}'_t), \quad (63)$$

where

$$\mathcal{A}'_t = A_{t,123.456}^{q,q} f_{t_r,123}^q \tilde{J}_{q\mu}^a(q_1, q_2) G^{\mu a}(q_3) f_{t_r,456}^q \tilde{J}_{q\nu}^b(q_4, q_5) G^{\nu b}(q_6), \quad (64)$$

$$\mathcal{B}'_t = A_{t,123.456}^{q,g} f_{t_r,123}^q \tilde{J}_{q\mu}^a(q_1, q_2) G^{\mu a}(q_3) f_{t_r,456}^g \tilde{J}_{g\nu}^b(q_4, q_5) G^{\nu b}(q_6), \quad (65)$$

$$\mathcal{C}'_t = A_{t,123.456}^{g,q} f_{t_r,123}^g \tilde{J}_{g\mu}^a(q_1, q_2) G^{\mu a}(q_3) f_{t_r,456}^q \tilde{J}_{q\nu}^b(q_4, q_5) G^{\nu b}(q_6), \quad (66)$$

$$\mathcal{D}'_t = A_{t,123.456}^{g,g} f_{t_r,123}^g \tilde{J}_{g\mu}^a(q_1, q_2) G^{\mu a}(q_3) f_{t_r,456}^g \tilde{J}_{g\nu}^b(q_4, q_5) G^{\nu b}(q_6), \quad (67)$$

and

$$A_{123.456}^{I,J} = (-Q_{123}^I + Q_{456}^J) \frac{f_{t,123}^I f_{t,456}^J}{f_{t,123456}^{I,J}}, \quad (68)$$

I	$a-g$	j	k	l	m	n
S_I	1	3	3	9	18	6

TABLE I. Symmetry factor S_I for diagram D_I .

for $I, J \in \{q, g\}$, where

$$Q_{ijk}^q = q_i^-|_m + q_j^-|_m + q_k^-|_{m_g}, \quad (69)$$

$$Q_{ijk}^g = q_i^-|_{m_g} + q_j^-|_{m_g} + q_k^-|_{m_g}, \quad (70)$$

$$f_{t,ijk}^J = e^{-t(Q_{ijk}^J)^2}, \quad (71)$$

$$f_{t,123456}^{I,J} = e^{-t(Q_{123}^I + Q_{456}^J)^2}. \quad (72)$$

The difference between various functions $A_{123,456}^{I,J}$ for various I and J is entirely contained in the difference between masses that enter the definitions of the minus components of various fourvectors q_i .

After integrating Eq. (63) over t we get,

$$h_{t,2} = h_{0,2} + \int [q_1 q_2 q_3 q_4 q_5 q_6] \tilde{\delta}_{123} \tilde{\delta}_{456} (\mathcal{A}_t + \mathcal{B}_t + \mathcal{C}_t + \mathcal{D}_t), \quad (73)$$

where

$$\mathcal{A}_t = \int_0^t d\tau \mathcal{A}'_\tau, \quad \text{etc.} \quad (74)$$

Therefore,

$$\mathcal{A}_t = B_{t,123,456}^{q,q} f_{t_r,123}^q \tilde{J}_{q\mu}^a(q_1, q_2) G^{\mu a}(q_3) f_{t_r,456}^q \tilde{J}_{q\nu}^b(q_4, q_5) G^{\nu b}(q_6), \quad (75)$$

$$\mathcal{B}_t = B_{t,123,456}^{q,g} f_{t_r,123}^q \tilde{J}_{q\mu}^a(q_1, q_2) G^{\mu a}(q_3) f_{t_r,456}^g \tilde{J}_{g\nu}^b(q_4, q_5) G^{\nu b}(q_6), \quad (76)$$

$$\mathcal{C}_t = B_{t,123,456}^{g,q} f_{t_r,123}^g \tilde{J}_{g\mu}^a(q_1, q_2) G^{\mu a}(q_3) f_{t_r,456}^q \tilde{J}_{q\nu}^b(q_4, q_5) G^{\nu b}(q_6), \quad (77)$$

$$\mathcal{D}_t = B_{t,123,456}^{g,g} f_{t_r,123}^g \tilde{J}_{g\mu}^a(q_1, q_2) G^{\mu a}(q_3) f_{t_r,456}^g \tilde{J}_{g\nu}^b(q_4, q_5) G^{\nu b}(q_6), \quad (78)$$

where

$$B_{123,456}^{I,J} = \frac{1}{2} \left(\frac{1}{Q_{123}^I} - \frac{1}{Q_{456}^J} \right) \left(\frac{f_{t,123}^I f_{t,456}^J}{f_{t,123456}^{I,J}} - 1 \right), \quad (79)$$

for $I, J \in \{q, g\}$.

Using Wick's theorem \mathcal{A}_t , \mathcal{B}_t , \mathcal{C}_t , and \mathcal{D}_t can be evaluated further. Equation (73) will be still correct if we make the following substitutions:

$$\mathcal{A}_t \rightarrow g^2 f_{t_r,123}^q f_{t_r,456}^q B_{t,123.456}^{q,q} (D_a + D_b + D_c + D_d + D_e + D_f + D_g) , \quad (80)$$

$$\mathcal{B}_t \rightarrow g^2 f_{t_r,123}^q f_{t_r,456}^g B_{t,123.456}^{q,g} S_j D_j , \quad (81)$$

$$\mathcal{C}_t \rightarrow g^2 f_{t_r,123}^g f_{t_r,456}^q B_{t,123.456}^{g,q} S_k D_k , \quad (82)$$

$$\mathcal{D}_t \rightarrow g^2 f_{t_r,123}^g f_{t_r,456}^g B_{t,123.456}^{g,g} (S_l D_l + S_m D_m + S_n D_n) , \quad (83)$$

where D_a, \dots, D_n represent Wick's contractions, are depicted in Figs. 3, 4, 5, 6, 7, 8, and 9, and are discussed in Sec. IV C and Sec. IV D. Formulas (80)–(83) are correct only under the integration sign of Eq. (73). \mathcal{B}_t , \mathcal{C}_t , and \mathcal{D}_t contain symmetry factors S_I , see Table I. In \mathcal{A}_t all symmetry factors are equal one and are omitted. For example, $S_j = 3$, because there are 3 similar diagrams that only differ by which of the three gluon legs of the right vertex is contracted with the unique gluon leg of the left vertex in Fig. 8. Since $F_{\alpha\beta\gamma}^{abc}(q_1, q_2, q_3)$ is symmetric with respect to simultaneous permutations $1 \rightarrow 2 \rightarrow 3 \rightarrow 1$, $a \rightarrow b \rightarrow c \rightarrow a$, and $\alpha \rightarrow \beta \rightarrow \gamma \rightarrow \alpha$, as well as simultaneous permutations $1 \leftrightarrow 2$, $a \leftrightarrow b$, and $\alpha \leftrightarrow \beta$, the three-gluon vertex is symmetric with respect to permutations of its legs and the three diagrams give the same result. Hence, instead of computing them separately, we can compute only one of them and multiply the result by 3. In another example, $S_m = 18$ because there are 3 choices of which two legs in diagram D_m should be contracted in the left vertex, 3 choices of which two legs should be contracted in the right vertex, and once these are chosen one still has 2 choices of how to contract two legs with two legs.

The reduced Hamiltonian becomes

$$h_{t,2} = h_{0,2} + \sum_{J \in \{a, \dots, n\}} h_{t,2}^{(J)} . \quad (84)$$

where $h_{t,2}^{(J)}$ for $J \in \{a, \dots, n\}$ come from Wick's contractions. $h_{0,2}$ contains the bare interaction vertices, meaning initial vertices at $t = 0$, and counterterms necessary to renormalize the theory,

$$h_{0,2} = H_{G^4} + H_{\psi^2 G^2} + H_{JJ} + X , \quad (85)$$

where X stands for the counterterms.

We discuss terms involving only quark-gluon vertices, i.e., diagrams D_a through D_g , in Sec. IV C. We discuss terms involving at least one three-gluon vertex, i.e., diagrams D_j through D_n , in Sec. IV D.

C. Wick's contractions involving only quark-gluon vertices

Diagrams D_a through D_g , depicted in Figs. 3–7, involve only quark-gluon vertices. These terms are analogous to the diagrams in Figs. 4(a)–(g) in the Yukawa paper. As compared to Yukawa paper, here the vertices involve Dirac gamma matrices, γ^μ or γ^ν , color matrices, T^a or T^b , and gluons carry a relativistic index, μ or ν , and a color index a or b . These differences come from the fact that quarks possess color charge, and gluons are vector bosons associated with the gauge group, as opposed to simple fermions and scalar bosons considered in the Yukawa paper. For the purpose of computing the effective Hamiltonians the differences are merely technical complications. Yukawa paper explains in much more detail the steps of the calculation. We summarize the results and recapitulate the most important comments.

Diagrams in Figs. 3 through 7 represent the following Wick's contractions:

$$D_a = \mathcal{N} \left[\overbrace{\bar{\Psi}(-q_1)\gamma_\mu T^a \Psi(q_2) G^{\mu a}(q_3) \bar{\Psi}(-q_4)\gamma_\nu T^b \Psi(q_5) G^{\nu b}(q_6)} \right], \quad (86)$$

$$D_b = \mathcal{N} \left[\overbrace{\bar{\Psi}(-q_1)\gamma_\mu T^a \Psi(q_2) G^{\mu a}(q_3) \bar{\Psi}(-q_4)\gamma_\nu T^b \Psi(q_5) G^{\nu b}(q_6)} \right], \quad (87)$$

$$D_c = \mathcal{N} \left[\overbrace{\bar{\Psi}(-q_1)\gamma_\mu T^a \Psi(q_2) G^{\mu a}(q_3) \bar{\Psi}(-q_4)\gamma_\nu T^b \Psi(q_5) G^{\nu b}(q_6)} \right], \quad (88)$$

$$D_d = \mathcal{N} \left[\overbrace{\bar{\Psi}(-q_1)\gamma_\mu T^a \Psi(q_2) G^{\mu a}(q_3) \bar{\Psi}(-q_4)\gamma_\nu T^b \Psi(q_5) G^{\nu b}(q_6)} \right], \quad (89)$$

$$D_e = \mathcal{N} \left[\overbrace{\bar{\Psi}(-q_1)\gamma_\mu T^a \Psi(q_2) G^{\mu a}(q_3) \bar{\Psi}(-q_4)\gamma_\nu T^b \Psi(q_5) G^{\nu b}(q_6)} \right], \quad (90)$$

$$D_f = \mathcal{N} \left[\overbrace{\bar{\Psi}(-q_1)\gamma_\mu T^a \Psi(q_2) G^{\mu a}(q_3) \bar{\Psi}(-q_4)\gamma_\nu T^b \Psi(q_5) G^{\nu b}(q_6)} \right], \quad (91)$$

$$D_g = \mathcal{N} \left[\overbrace{\bar{\Psi}(-q_1)\gamma_\mu T^a \Psi(q_2) G^{\mu a}(q_3) \bar{\Psi}(-q_4)\gamma_\nu T^b \Psi(q_5) G^{\nu b}(q_6)} \right]. \quad (92)$$

The contractions are

$$\overbrace{\bar{\Psi}_{a_1 c_1}(-q_1) \Psi_{a_2 c_2}(q_2)} = \frac{\theta(q_1^+)}{|q_1^+|} \tilde{\delta}(q_1 + q_2) \delta_{c_2, c_1} (\not{q}_1 - m)_{a_2, a_1}, \quad (93)$$

$$\overbrace{\bar{\Psi}_{a_1 c_1}(q_1) \Psi_{a_2 c_2}(-q_2)} = \frac{\theta(q_1^+)}{|q_1^+|} \tilde{\delta}(q_1 + q_2) \delta_{c_1, c_2} (\not{q}_1 + m)_{a_1, a_2}, \quad (94)$$

$$\overbrace{G^{\mu a}(q_1) G^{\nu b}(q_2)} = \frac{\theta(q_1^+)}{|q_1^+|} \tilde{\delta}(q_1 + q_2) \delta_{ab} d^{\mu\nu}(q_1), \quad (95)$$

where indices $a_1, a_2 = 1, 2, 3, 4$ enumerate entries in the spinor space, while indices $c_1, c_2 = 1, 2, 3$ enumerate entries in the color space of the quark field. The polarization tensor is

$$d^{\mu\nu}(q) = -g^{\mu\nu} + \frac{n^\mu q^\nu + n^\nu q^\mu}{q^+} - n^\mu n^\nu \frac{q^2}{(q^+)^2}, \quad (96)$$

Note that $q^- = [m_g^2 + (q^\perp)^2]/q^+$. Therefore, $q^2 = m_g^2$, and $d^{\mu\nu}(q)$ depends only on q^+ and q^\perp , and does not depend on m_g . Explicitly,

$$d^{--}(q) = \frac{4(q^\perp)^2}{(q^+)^2}, \quad (97)$$

$$d^{ij}(q) = \delta^{ij}, \quad (98)$$

$$d^{-i}(q) = d^{i-}(q) = \frac{2q^i}{q^+}, \quad (99)$$

$$d^{+\nu}(q) = d^{\nu+}(q) = 0. \quad (100)$$

For $J \in \{a, \dots, g\}$

$$h_{t,2}^{(J)} = g^2 \int [q_1 q_2 q_3 q_4 q_5 q_6] \tilde{\delta}_{123} \tilde{\delta}_{456} f_{t_r,123}^q f_{t_r,456}^q B_{t,123,456}^{q,q} D_J. \quad (101)$$

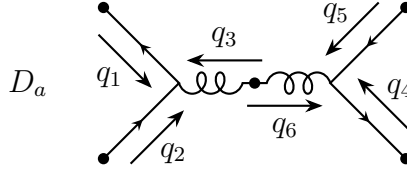


FIG. 3. Wick's diagram D_a .

Diagram D_a , Fig. 3 gives,

$$h_{t,2}^{(a)} = g^2 \int [q_1 q_2 q_3 q_4 q_5] \tilde{\delta}_{123} \tilde{\delta}_{45,3} f_{t_r,123}^q f_{t_r,45,3}^q B_{t,123,45(-3)}^{q,q} \frac{\theta(q_3^+)}{q_3^+} \times d^{\mu\nu}(q_3) \mathcal{N} [\bar{\Psi}(-q_1) \gamma_\mu T^a \Psi(q_2) \bar{\Psi}(-q_4) \gamma_\nu T^a \Psi(q_5)]. \quad (102)$$

Diagrams D_b and D_c , Fig. 4 give,

$$h_{t,2}^{(b)} + h_{t,2}^{(c)} = g^2 \int [q_1 q_2 q_3 q_5 q_6] \tilde{\delta}_{123} \tilde{\delta}_{56,2} f_{t_r,123}^q f_{t_r,(-2)56}^q B_{t,123,(-2)56}^{q,q} \frac{1}{q_2^+} \times \mathcal{N} [\bar{\Psi}(-q_1) \gamma_\mu T^a G^{\mu a}(q_3) (\not{q}_2 + m) \gamma_\nu T^b G^{\nu b}(q_6) \Psi(q_5)]. \quad (103)$$

Diagrams D_d and D_e , Fig. 5 give,

$$h_{t,2}^{(d)} + h_{t,2}^{(e)} = C_F g^2 \int [q_1 q_2 q_3] \tilde{\delta}_{23,1} \frac{B_{t,(-1)23,1(-2)(-3)}^{q,q}}{|q_2^+ q_3^+|} (f_{t_r,(-1)23}^q)^2 \times d^{\mu\nu}(q_3) \mathcal{N} [\bar{\Psi}(q_1) \gamma_\mu (\not{q}_2 + m) \gamma_\nu \Psi(q_1)] [\theta(q_2^+) \theta(q_3^+) - \theta(-q_2^+) \theta(-q_3^+)], \quad (104)$$

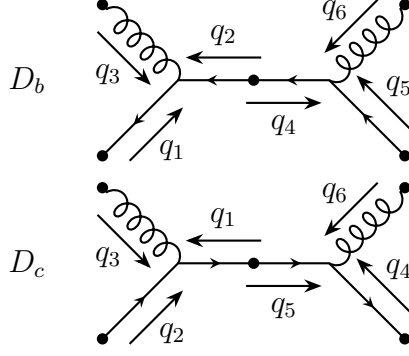


FIG. 4. Wick's diagrams D_b and D_c .

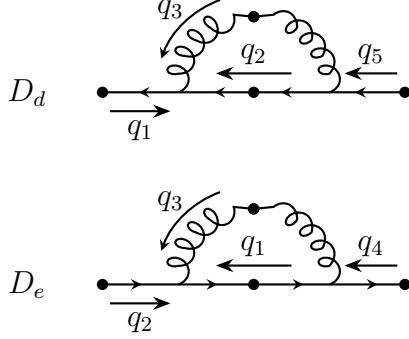


FIG. 5. Wick's diagrams D_d and D_e .

where

$$B_{t,(-1)23,1(-2)(-3)}^{q,q} = \frac{(f_{t,(-1)23}^q)^2 - 1}{q_2^-|_m + q_3^-|_{m_g} - q_1^-|_m}, \quad (105)$$

and $C_F = (N_c^2 - 1)/(2N_c) = 4/3$ for the number of colors $N_c = 3$. Using the Gordon identity,

$$h_{t,2}^{(d)} + h_{t,2}^{(e)} = \int [q] \frac{\delta \tilde{m}_{t,2}^2}{q^+} \mathcal{N} \left[\bar{\Psi}(q) \frac{\gamma^+}{2} \Psi(q) \right], \quad (106)$$

where

$$\begin{aligned} \delta \tilde{m}_{t,2}^2 &= C_F g^2 \int [q_2 q_3] \tilde{\delta}_{23,q} \frac{B_{t,(-q)23,q(-2)(-3)}^{q,q}}{q_2^+ q_3^+} (f_{t_r,(-q)23}^q)^2 \theta(q_2^+) \theta(q_3^+) \\ &\times d_{\mu\nu}(q_3) \bar{u}_\sigma(q) \gamma^\mu (\not{q}_2 + m) \gamma^\nu u_\sigma(q). \end{aligned} \quad (107)$$

Diagram D_f , Fig. 6 gives,

$$h_{t,2}^{(f)} = \int [q_3] \theta(q_3^+) \tilde{\Pi}_{\mu\nu}^q(q_3) \mathcal{N} [G^{\mu a}(-q_3) G^{\nu a}(q_3)], \quad (108)$$

where

$$\begin{aligned} \tilde{\Pi}_{\mu\nu}^q(q_3) &= g^2 \int [q_1 q_2] \tilde{\delta}_{12,3} \frac{\theta(q_1^+) \theta(q_2^+)}{|q_1^+| |q_2^+|} B_{t,12(-3),(-1)(-2)3}^{q,q} (f_{t_r,12(-3)}^q)^2 \\ &\times T_f \text{Tr} \left[\gamma_\mu (\not{q}_2 + m) \gamma_\nu (\not{q}_1 - m) \right], \end{aligned} \quad (109)$$

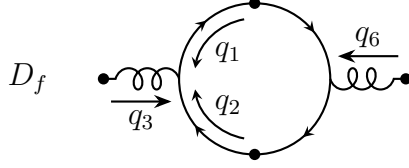


FIG. 6. Wick's diagram D_f .

with $T_f = \frac{1}{2}$, and

$$B_{t,12(-3).(-1)(-2)3}^{q,q} = \frac{(f_{t,12(-3)}^q)^2 - 1}{q_1^- + q_2^- - q_3^-}. \quad (110)$$

$\tilde{\Pi}_{\mu\nu}^q(q_3)$ is to some extent similar to vacuum polarization tensor as defined in calculations of correlation functions, but should not be confused with it. $\tilde{\Pi}_{\mu\nu}^q(q_3)$ is just a part of the expression for the effective Hamiltonian, and as such it will be an ingredient of a calculation of the effective vacuum polarization. Only components $\mu, \nu = -, 1, 2$ contribute to Eq. (108), because $G^{+a}(q) = 0$ due to gauge choice, and they satisfy relations,

$$\tilde{\Pi}_{-i}^q(q_3) = \tilde{\Pi}_{i-}^q(q_3) = -\tilde{\Pi}_{--}^q(q_3) \frac{2q_3^i}{q_3^+}, \quad (111)$$

$$\tilde{\Pi}_{ij}^q(q_3) = \tilde{\Pi}_{--}^q(q_3) \frac{4q_3^i q_3^j}{(q_3^+)^2} + \delta_{ij} \delta \tilde{\mu}_{t,q,2}^2(q_3), \quad (112)$$

where

$$\tilde{\Pi}_{--}^q(q_3) = T_f g^2 \int [q_1 q_2] \frac{\theta(q_1^+) \theta(q_2^+)}{|q_1^+| |q_2^+|} \tilde{\delta}_{12.3} B_{t,12(-3).(-1)(-2)3}^{q,q} (f_{t,12(-3)}^q)^2 \cdot 2q_1^+ q_2^+, \quad (113)$$

$$\delta \tilde{\mu}_{t,q,2}^2(q_3) = 2T_f g^2 \int [q_1 q_2] \frac{\theta(q_1^+) \theta(q_2^+)}{|q_1^+| |q_2^+|} \tilde{\delta}_{12.3} B_{t,12(-3).(-1)(-2)3}^{q,q} (f_{t,12(-3)}^q)^2 [\mathcal{M}_{12}^2 - 2k^2], \quad (114)$$

with $\mathcal{M}_{12}^2 = \frac{m^2 + k^2}{x_1 x_2}$. $k^\perp = (k^1, k^2)$ and $x_1 = q_1^+ / q_3^+ = 1 - x_2$, are relative momentum variables, such that

$$q_1^i = k^i + x_1 q_3^i, \quad (115)$$

$$q_2^i = -k^i + x_2 q_3^i. \quad (116)$$

For simplicity, $k^2 = (k^\perp)^2$, not to be confused with k^2 as the second coordinate of k^\perp . Relations (111) and (112) can be checked explicitly using,

$$\text{Tr} \left[\gamma_\mu (\not{q}_2 + m) \gamma_\nu (\not{q}_1 - m) \right] = 4q_{1\mu} q_{2\nu} + 4q_{1\nu} q_{2\mu} - 4g_{\mu\nu} (q_1 \cdot q_2 + m^2). \quad (117)$$

Any term that is linear in k^1 , k^2 , or $k^1 k^2$, integrates to zero in Eq. (109), because all other factors of the integrand depend on $(k^\perp)^2$. In particular this means that $k^i k^j$ can be replaced under the integral with $\delta_{ij}(k^\perp)^2/2$, which leads to Eq. (112).

Since $q_\mu G^{\mu a}(q) = 0$,

$$G^{-a}(q) = \frac{2q^j G^{ja}(q)}{q^+}, \quad (118)$$

and one can express Eq. (109) in terms of $G^{ia}(q)$ only. Using Eqs. (111) and (112), we obtain

$$h_{t,2}^{(f)} = \int [q_3] \theta(q_3^+) \delta \tilde{\mu}_{t,q,2}^2(q_3) \mathcal{N} [G^{ia}(-q_3) G^{ia}(q_3)], \quad (119)$$

where only $\delta \tilde{\mu}_{t,q,2}^2(q_3)$ contributes, while all instances of $\tilde{\Pi}_{--}^q(q_3)$ canceled each other. Comparison with Eq. (29) reveals that $\delta \tilde{\mu}_{t,q,2}^2(q_3)$ is a correction to the free gluon mass m_g .

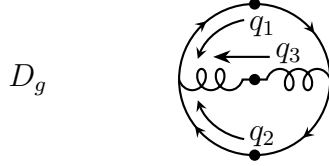


FIG. 7. Wick's diagram D_g .

Finally, diagram D_g , Fig. 7 gives,

$$h_{t,2}^{(g)} = 0, \quad (120)$$

due to the small longitudinal momentum cutoff.

D. Wick's contractions involving triple gluon vertices

Diagram D_j , Fig. 8 gives,

$$h_{t,2}^{(j)} = g^2 \int [q_1 q_2 q_3 q_4 q_5 q_6] \tilde{\delta}_{123} \tilde{\delta}_{456} f_{t_r,123}^q f_{t_r,456}^g B_{t,123,456}^{q,g} \cdot 3D_j, \quad (121)$$

where

$$D_j = \frac{1}{3!} F_{\alpha\beta\gamma}^{abc}(q_4, q_5, q_6) \mathcal{N} \left[\bar{\Psi}(-q_1) \gamma_\mu T^d \Psi(q_2) \overbrace{G^{\mu d}(q_3) G^{\alpha a}(q_4) G^{\beta b}(q_5) G^{\gamma c}(q_6)} \right]. \quad (122)$$

Therefore,

$$\begin{aligned} h_{t,2}^{(j)} &= g^2 \int [q_1 q_2 q_3 q_4 q_5] \tilde{\delta}_{123} \tilde{\delta}_{45,3} f_{t_r,123}^q f_{t_r,45(-3)}^g B_{t,123,45(-3)}^{q,g} \frac{\theta(q_3^+)}{|q_3^+|} \\ &\times d^{\mu\gamma}(q_3) \frac{1}{2} F_{\alpha\beta\gamma}^{abc}(q_4, q_5, -q_3) \mathcal{N} \left[\bar{\Psi}(-q_1) \gamma_\mu T^c \Psi(q_2) G^{\alpha a}(q_4) G^{\beta b}(q_5) \right]. \end{aligned} \quad (123)$$

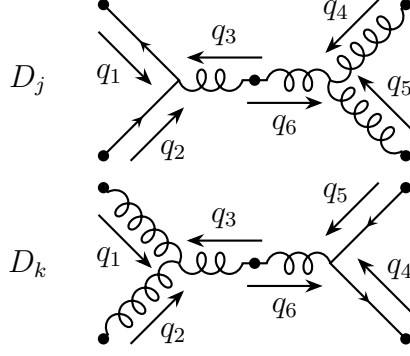


FIG. 8. Wick's diagrams D_j and D_k .

Similarly, diagram D_k , Fig. 8 gives,

$$h_{t,2}^{(k)} = g^2 \int [q_1 q_2 q_3 q_4 q_5 q_6] \tilde{\delta}_{123} \tilde{\delta}_{456} f_{t_r,123}^g f_{t_r,456}^q B_{t,123.456}^{g,q} \cdot 3D_k, \quad (124)$$

where

$$D_k = \frac{1}{3!} F_{\alpha\beta\gamma}^{abc}(q_1, q_2, q_3) \mathcal{N} \left[G^{\alpha\alpha}(q_1) G^{\beta\beta}(q_2) \overline{G^{\gamma\gamma}(q_3) \bar{\Psi}(-q_4) \gamma_\mu T^d \Psi(q_5) G^{\mu d}(q_6)} \right]. \quad (125)$$

Therefore,

$$\begin{aligned} h_{t,2}^{(k)} &= g^2 \int [q_1 q_2 q_3 q_4 q_5] \tilde{\delta}_{123} \tilde{\delta}_{45.3} f_{t_r,123}^g f_{t_r,45(-3)}^q B_{t,123.45(-3)}^{g,q} \frac{\theta(q_3^+)}{|q_3^+|} \\ &\times d^{\gamma\mu}(q_3) \frac{1}{2} F_{\alpha\beta\gamma}^{abc}(q_1, q_2, q_3) \mathcal{N} \left[G^{\alpha\alpha}(q_1) G^{\beta\beta}(q_2) \bar{\Psi}(-q_4) \gamma_\mu T^c \Psi(q_5) \right]. \end{aligned} \quad (126)$$

Substituting $q_3 \rightarrow -q_3$, relabeling $1 \leftrightarrow 4$, and $2 \leftrightarrow 5$, then shifting $G^{\alpha\alpha}(q_4) G^{\beta\beta}(q_5)$ to the right under the normal ordering sign, finally using symmetries $d^{\mu\gamma}(-q_3) = d^{\mu\gamma}(q_3)$, and $B_{t,45(-3).123}^{g,q} = -B_{t,123.45(-3)}^{g,q}$, $h_{t,2}^{(k)}$ is rewritten in a form almost identical to that of $h_{t,2}^{(j)}$. The only difference is that where $h_{t,2}^{(j)}$ has $\theta(q_3^+)$, $h_{t,2}^{(k)}$ has $-\theta(-q_3^+)$. Since $\theta(q_3^+) - \theta(-q_3^+) = \text{sign}(q_3^+)$, the sum becomes

$$\begin{aligned} h_{t,2}^{(j)} + h_{t,2}^{(k)} &= g^2 \int [q_1 q_2 q_3 q_4 q_5] \tilde{\delta}_{123} \tilde{\delta}_{45.3} f_{t_r,123}^q f_{t_r,45(-3)}^g B_{t,123.45(-3)}^{q,g} \frac{1}{q_3^+} \\ &\times d^{\mu\gamma}(q_3) \frac{1}{2} F_{\alpha\beta\gamma}^{abc}(q_4, q_5, -q_3) \mathcal{N} \left[\bar{\Psi}(-q_1) \gamma_\mu T^c \Psi(q_2) G^{\alpha\alpha}(q_4) G^{\beta\beta}(q_5) \right]. \end{aligned} \quad (127)$$

For $J \in \{l, m, n\}$

$$h_{t,2}^{(J)} = g^2 \int [q_1 q_2 q_3 q_4 q_5 q_6] \tilde{\delta}_{123} \tilde{\delta}_{456} f_{t_r,123}^g f_{t_r,456}^q B_{t,123.456}^{g,q} S_J D_J. \quad (128)$$

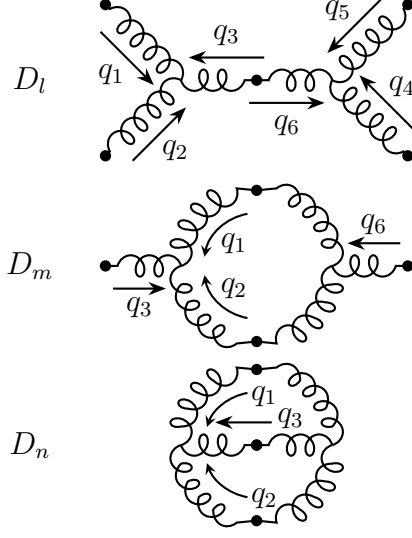


FIG. 9. Wick's diagrams D_l , D_m , and D_n .

Diagrams D_l , D_m , and D_n , Fig. 9 are,

$$D_l = \frac{1}{3!} F_{\alpha\beta\gamma}^{abc}(q_1, q_2, q_3) \frac{1}{3!} F_{\mu\nu\rho}^{def}(q_4, q_5, q_6) \times \mathcal{N} \left[\overbrace{G^{\alpha\alpha}(q_1) G^{\beta\beta}(q_2) G^{\gamma c}(q_3) G^{\mu d}(q_4) G^{\nu e}(q_5) G^{\rho f}(q_6)} \right], \quad (129)$$

$$D_m = \frac{1}{3!} F_{\alpha\beta\gamma}^{abc}(q_1, q_2, q_3) \frac{1}{3!} F_{\mu\nu\rho}^{def}(q_4, q_5, q_6) \times \mathcal{N} \left[\overbrace{G^{\alpha\alpha}(q_1) G^{\beta\beta}(q_2) G^{\gamma c}(q_3) G^{\mu d}(q_4) G^{\nu e}(q_5) G^{\rho f}(q_6)} \right]. \quad (130)$$

$$D_n = \frac{1}{3!} F_{\alpha\beta\gamma}^{abc}(q_1, q_2, q_3) \frac{1}{3!} F_{\mu\nu\rho}^{def}(q_4, q_5, q_6) \times \mathcal{N} \left[\overbrace{G^{\alpha\alpha}(q_1) G^{\beta\beta}(q_2) G^{\gamma c}(q_3) G^{\mu d}(q_4) G^{\nu e}(q_5) G^{\rho f}(q_6)} \right]. \quad (131)$$

Therefore,

$$h_{t,2}^{(l)} = g^2 \int [q_1 q_2 q_3 q_4 q_5] \tilde{\delta}_{123} \tilde{\delta}_{45,3} f_{t_r,123}^g f_{t_r,45(-3)}^g B_{t,123,45(-3)}^{g,g} \frac{\theta(q_3^+)}{|q_3^+|} \times \frac{1}{2} F_{\alpha\beta\gamma}^{abc}(q_1, q_2, q_3) \frac{1}{2} F_{\mu\nu\rho}^{dec}(q_4, q_5, -q_3) \times d^{\gamma\rho}(q_3) \mathcal{N} [G^{\alpha\alpha}(q_1) G^{\beta\beta}(q_2) G^{\mu d}(q_4) G^{\nu e}(q_5)], \quad (132)$$

$$h_{t,2}^{(m)} = \frac{1}{2} g^2 \int [q_1 q_2 q_3] \tilde{\delta}_{12,3} f_{t_r,12(-3)}^g f_{t_r,(-1)(-2)3}^g B_{t,12(-3),(-1)(-2)3}^{g,g} \frac{\theta(q_1^+) \theta(q_2^+)}{|q_1^+| |q_2^+|} \times F_{\alpha\beta\gamma}^{abc}(q_1, q_2, -q_3) F_{\mu\nu\rho}^{abf}(-q_1, -q_2, q_3) d^{\alpha\mu}(q_1) d^{\beta\nu}(q_2) \mathcal{N} [G^{\gamma c}(-q_3) G^{\rho f}(q_3)], \quad (133)$$

$$h_{t,2}^{(n)} = 0, \quad (134)$$

where $h_{t,2}^{(n)}$ is zero because of small longitudinal momentum cutoff.

Since $f^{abc}f^{abf} = C_A\delta^{cf}$, where $C_A = N_c$, the gluon mass term can be written as

$$h_{t,2}^{(m)} = \int [q_3] \theta(q_3^+) \tilde{\Pi}_{\mu\nu}^g(q_3) \mathcal{N} [G^{\mu a}(-q_3) G^{\nu a}(q_3)], \quad (135)$$

where

$$\begin{aligned} \tilde{\Pi}_{\mu\nu}^g(q_3) &= \frac{1}{2} C_A g^2 \int [q_1 q_2] \tilde{\delta}_{12.3}(f_{t_r,12(-3)}^g)^2 B_{t,12(-3).(-1)(-2)3}^{g.g} \frac{\theta(q_1^+) \theta(q_2^+)}{|q_1^+| |q_2^+|} \\ &\times d^{\alpha\gamma}(q_1) [(q_{2\mu} - q_{1\mu})g_{\alpha\beta} - (q_{3\alpha} + q_{2\alpha})g_{\beta\mu} + (q_{1\beta} + q_{3\beta})g_{\mu\alpha}] \\ &\times d^{\beta\delta}(q_2) [(q_{2\nu} - q_{1\nu})g_{\gamma\delta} - (q_{3\gamma} + q_{2\gamma})g_{\delta\nu} + (q_{1\delta} + q_{3\delta})g_{\nu\gamma}]. \end{aligned} \quad (136)$$

Analogously to $\tilde{\Pi}_{\mu\nu}^g$, with a use of Eqs. (115) and (116), we find,

$$\tilde{\Pi}_{-i}^g(q_3) = \tilde{\Pi}_{i-}^g(q_3) = -\tilde{\Pi}_{--}^g(q_3) \frac{2q_3^i}{q_3^+}. \quad (137)$$

$$\tilde{\Pi}_{ij}^g(q_3) = \tilde{\Pi}_{--}^g(q_3) \frac{4q_3^i q_3^j}{(q_3^+)^2} + \delta_{ij} \delta\tilde{\mu}_{t,g,2}^2(q_3), \quad (138)$$

where

$$\tilde{\Pi}_{--}^g(q_3) = C_A g^2 \int [q_1 q_2] \tilde{\delta}_{12.3}(f_{t_r,12(-3)}^g)^2 B_{t,12(-3).(-1)(-2)3}^{g.g} \frac{\theta(q_1^+) \theta(q_2^+) (q_2^+ - q_1^+)^2}{|q_1^+| |q_2^+| 4}. \quad (139)$$

$$\delta\tilde{\mu}_{t,g,2}^2(q_3) = C_A g^2 \int [q_1 q_2] \tilde{\delta}_{12.3}(f_{t_r,12(-3)}^g)^2 B_{t,12(-3).(-1)(-2)3}^{g.g} \frac{\theta(q_1^+) \theta(q_2^+)}{|q_1^+| |q_2^+|} \cdot 2(k^+)^2 \frac{(1 - x_1 x_2)^2}{(x_1 x_2)^2}. \quad (140)$$

Therefore,

$$h_{t,2}^{(m)} = \int [q_3] \theta(q_3^+) \delta\tilde{\mu}_{t,g,2}^2(q_3) \mathcal{N} [G^{ia}(-q_3) G^{ia}(q_3)], \quad (141)$$

and $\delta\tilde{\mu}_{t,g,2}^2(q_3)$ is the second-order contribution to the gluon mass term in the Hamiltonian that comes from the gluon loop.

V. COUNTERTERMS

In this section we study the $t_r \rightarrow 0$ limit and find counterterms that make this limit well defined. The rule for finding the counterterms is to ensure that all matrix elements of the effective Hamiltonians are well defined in the $t_r \rightarrow 0$ limit. We retain a finite gluon mass while taking $t_r \rightarrow 0$ which ensures that all matrix elements, even those outside the color

singlet sector, are finite. We then take $m_g \rightarrow 0$ in Sec. VI. In the limit $t_r \rightarrow 0$, $m_g \rightarrow 0$ we only expect the matrix elements in the color singlet sector to remain finite.

The Hamiltonian of QCD is an unbounded operator that acts on an infinite-dimensional Hilbert space. Such an operator cannot be well defined on the whole of Hilbert space but at most on a dense subspace of it. Therefore, a mathematically rigorous definition of the Hamiltonian requires us to provide its domain. Simply put, a matrix element is formed from an operator and two states, and so finiteness of matrix elements depends on the set of states one is allowed to consider, i.e. the domain of the operator. Loosely speaking, the Hilbert space in which we work is the Fock space build by quark and gluon creation operators, $b_{p\sigma c}^\dagger$, $d_{p\sigma c}^\dagger$, and $a_{p\sigma c}^\dagger$, on top of the free vacuum state $|0\rangle$. Due to commutation and anticommutation relations between these operators, the states have the proper symmetries required by indistinguishability.

We define a subspace, F_0 of the Fock space to be the space of vectors that have nonzero components in finitely many Fock sectors whose wave functions have compact support assuming that the longitudinal momenta, p^+ belong to the open set $(0, \infty)$. This means in particular that the wave functions are zero for momenta of particles that are larger than some finite number or their longitudinal momenta are smaller than some positive number. Effectively, longitudinal momentum of each particle is limited from below by some $\epsilon^+ > 0$, except that ϵ^+ depends now on the wave function in question. The universal, positive ϵ^+ that limited the longitudinal momenta in interaction terms of the Hamiltonian is at this point removed. Henceforth, we choose F_0 for the domain of the Hamiltonians.

The ultimate goal is to define a Hamiltonian that is a self-adjoint operator. Often the first step is to define an operator that is symmetric and then to seek its self-adjoint extensions. The Hamiltonians that we calculate will be proved to be well-defined symmetric forms with F_0 as the domain, i.e., their matrix elements exist. It is reasonable to expect that these forms correspond to symmetric operators. Finding self-adjoint extensions of these symmetric operators is a technically challenging task and we do not attempt it here. Nevertheless, the statement of the problem itself is valuable and, to our knowledge, novel. In particular, the problem of zero modes is reinterpreted as closely related to the problem of finding self-adjoint extensions of symmetric operators.

A generic state with R quarks, S antiquarks, and $n - R - S$ gluons can be written as

$$|\psi\rangle = \sum_{\text{discrete}} \int [p_1 \cdots p_n] \psi_{\text{discrete}}(p_1, \dots, p_n) \left(\prod_{k=1}^n \frac{\theta(p_k^+)}{p_k^+} q_k^\dagger \right) |0\rangle, \quad (142)$$

where, $q_k = b_k$ for $1 \leq k \leq R$, $q_k = d_k$ for $R + 1 \leq k \leq R + S$, and $q_k = a_k$ for $R + S + 1 \leq k \leq n$.

The contractions of these states with various operators are as follows:

$$\overline{\Psi}(q) b_{p\lambda c}^\dagger = \tilde{\delta}_{q,p} \theta_\epsilon(p^+) \chi_c u_\lambda(p), \quad (143)$$

$$\overline{\Psi}(-q) d_{p\lambda c}^\dagger = \tilde{\delta}_{q,p} \theta_\epsilon(p^+) \bar{v}_\lambda(p) \chi_c^\dagger, \quad (144)$$

$$\overline{G^{\mu a}}(q) a_{p\lambda c}^\dagger = \tilde{\delta}_{q,p} \theta_\epsilon(p^+) \delta_{ac} \varepsilon_\lambda^\mu(p), \quad (145)$$

$$\overline{b_{p\lambda c}} \overline{\Psi}(-q) = \tilde{\delta}_{qp} \theta_\epsilon(p^+) \bar{u}_\lambda(p) \chi_c^\dagger, \quad (146)$$

$$\overline{d_{p\lambda c}} \overline{\Psi}(q) = \delta_{qp} \theta_\epsilon(p^+) \chi_c v_\lambda(p), \quad (147)$$

$$\overline{a_{p\lambda c}} \overline{G^{\mu a}}(q) = \tilde{\delta}_{qp} \theta_\epsilon(p^+) \delta_{ac} \varepsilon_\lambda^{\mu*}(p), \quad (148)$$

where

$$\varepsilon_\sigma^i(q) = \varepsilon_\sigma^i, \quad (149)$$

$$\varepsilon_\sigma^-(q) = \frac{2q^i \varepsilon_\sigma^i}{q^+}, \quad (150)$$

$$u_\sigma(p) = \begin{bmatrix} \sqrt{p^+} \xi_\sigma \\ \frac{i\sigma^\perp \times p^\perp + m}{\sqrt{p^+}} \xi_\sigma \end{bmatrix}, \quad (151)$$

and $\sigma^\perp \times p^\perp = \sigma^1 p^2 - \sigma^2 p^1$.

One can see that contractions between Hamiltonian terms and states introduce spinors or polarization vectors and potentially some singular $1/q^+$ or $1/\sqrt{q^+}$ factors, but these singularities, so called endpoint singularities, are regulated by the compactness of the wave functions. In particular, compactness implies that the support of the integrand is bounded. Therefore, the only way a matrix element can diverge is when the interaction kernel becomes unbounded as $t_r \rightarrow 0$. For example, the whole kernel can be shifted to infinity as t_r approaches zero. Another exemplary possibility is that the kernel approaches a function of the form $1/(q^+)^2$, which is not integrable, as t_r approaches zero. Both examples are

found in the effective QCD Hamiltonian and we discuss them below. With the understanding that the wave functions regulate endpoint singularities we can study the Hamiltonian terms themselves instead of their matrix elements. Therefore, our analysis can be slightly simplified.

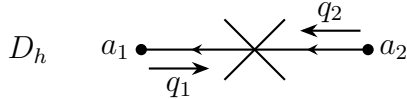


FIG. 10. Wick's diagram for the fermion mass counterterm.

First, we discuss the quark self-energy terms that arise from diagrams D_d and D_e , Fig. 5, Eq. (104). $\delta\tilde{m}_{t,2}^2$ diverges as $t_r \rightarrow 0$, leading to diverging matrix elements. Hence, one needs to add a mass counterterm. $\delta\tilde{m}_{t,2}^2$ is defined with $B_{t,(-1)23.1(-2)(-3)}^{q,q}$, Eq. (105) in the integrand. If the numerator of $B_{t,(-1)23.1(-2)(-3)}^{q,q}$ were just the form factor, $(f_{t,(-1)23}^q)^2$, then the integral would be finite in the $t_r \rightarrow 0$ limit. It is the -1 term in the numerator of $B_{t,(-1)23.1(-2)(-3)}^{q,q}$ that leads to a divergent integral. To counter this divergence we add a counterterm,

$$\mathcal{H}_{t,2}^{(h)} = \int [q] \frac{\delta m_{t,X,2}^2}{q^+} \mathcal{N} \left[\bar{\Psi}(q) \frac{\gamma^+}{2} \Psi(q) \right], \quad (152)$$

where

$$\begin{aligned} \delta m_{t,X,2}^2 = & C_F g^2 \int [q_2 q_3] \tilde{\delta}_{23,q} \frac{\theta(q_2^+) \theta(q_3^+)}{q_2^+ q_3^+} \frac{(f_{t_r,(-q)23}^q)^2}{q_2^-|_m + q_3^-|_{m_g} - q_1^-|_m} \\ & \times d_{\mu\nu}(q_3) \bar{u}_\sigma(q) \gamma^\mu (\not{q}_2 + m) \gamma^\nu u_\sigma(q) + \delta m_{\text{finite},2}^2. \end{aligned} \quad (153)$$

The counterterm is represented as a Wick's diagram in Fig. 10. The first term of $\delta m_{t,X,2}^2$ is divergent as $t_r \rightarrow 0$ and cancels the divergent part of the integrand in Eq. (107). The second term, $\delta m_{\text{finite},2}^2$ is assumed independent of t_r and is added because a priori we do not know what the finite part of the counterterm should be. We discuss the choice of the finite part in Sec. VII.

Next, we discuss the gluon self-energy terms that arise from diagrams D_f and D_m , Figs. 6 and 9, Eqs. (119) and (141), respectively. Both $\delta\tilde{\mu}_{t,q,2}^2$ and $\delta\tilde{\mu}_{t,g,2}^2$ diverge as $t_r \rightarrow 0$, and the divergence can be traced to the -1 term in the numerator of $B_{t,12(-3),(-1)(-2)3}^{q,q}$ and

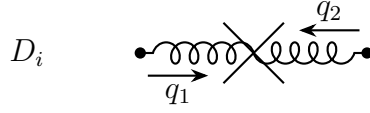


FIG. 11. Wick's diagram for the gluon mass counterterm.

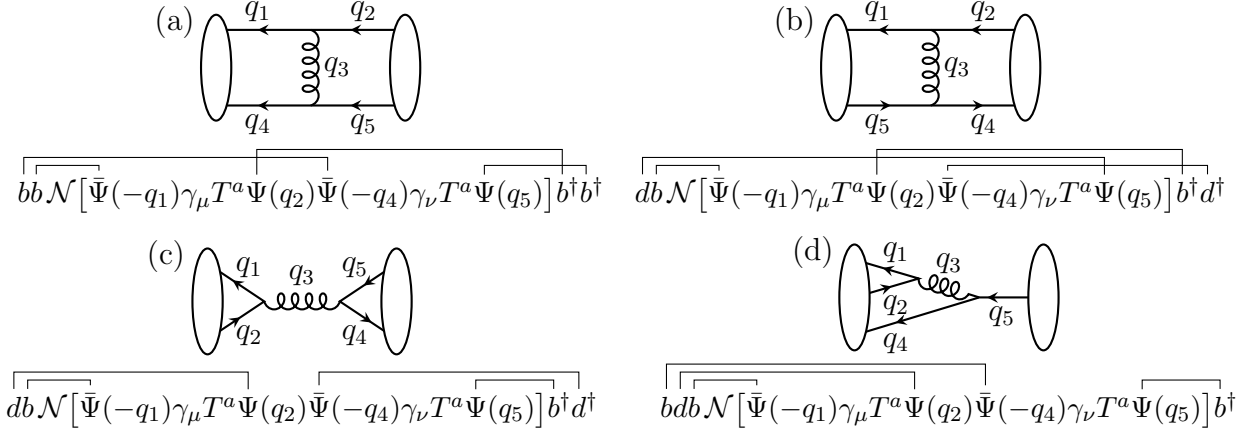


FIG. 12. Exemplary matrix elements of $\mathcal{H}_{t,2}^{(a)}$.

$B_{t,12(-3).(-1)(-2)3}^{g:g}$, respectively. Therefore, similarly to the quark case, we define a counterterm,

$$\mathcal{H}_{t,2}^{(i)} = \int [q_3] \theta(q_3^+) \delta \tilde{\mu}_{t,X,2}^2(q_3) \mathcal{N} [G^{ia}(-q_3) G^{ia}(q_3)], \quad (154)$$

where

$$\begin{aligned} \delta \tilde{\mu}_{t,X,2}^2(q_3) &= 2T_f g^2 \int [q_1 q_2] \frac{\theta(q_1^+) \theta(q_2^+)}{q_1^+ q_2^+} \tilde{\delta}_{12.3} \frac{(f_{t_r,12(-3)}^q)^2}{q_1^-|_m + q_2^-|_m - q_3^-|_{m_g}} [\mathcal{M}_{12}^2 - 2(k^\perp)^2] \\ &+ C_A g^2 \int [q_1 q_2] \frac{\theta(q_1^+) \theta(q_2^+)}{q_1^+ q_2^+} \tilde{\delta}_{12.3} \frac{(f_{t_r,12(-3)}^g)^2}{q_1^-|_{m_g} + q_2^-|_{m_g} - q_3^-|_{m_g}} 2(k^\perp)^2 \frac{(1-x_1 x_2)^2}{(x_1 x_2)^2} \\ &+ \delta \mu_{\text{finite},2}^2. \end{aligned} \quad (155)$$

The counterterm is represented as a Wick's diagram in Fig. 11. The first term of $\delta \tilde{\mu}_{t,X,2}^2(q_3)$ cancels the divergence as $t_r \rightarrow 0$ of the quark loop self-energy, Fig. 6, and the second term cancels the divergence of the gluon loop self-energy, Fig. 9. $\delta \mu_{\text{finite},2}^2$ is the finite part of the gluon mass counterterm, discussed in Sec. VII.

Terms $\mathcal{H}_{t,2}^{(I)}$ for $I \in \{a, j, k, l\}$, corresponding to diagrams, Figs. 3, 8, and 9 have very

I	a	j	k	l
K	q	q	g	g
L	q	g	q	g

TABLE II. For a given label (diagram) I , labels K and L are determined from this table.

similar form, and can be written,

$$\mathcal{H}_{t,2}^{(I)} = \frac{S_I}{2} \int [q_1 q_2 q_3 q_4 q_5] \tilde{\delta}_{123} \tilde{\delta}_{45.3} f_{t_r,123}^K f_{t_r,45(-3)}^L \times \frac{f_{t,1245}^{K.L} B_{t,123.45(-3)}^{K.L}}{q_3^+} d_{\mu\nu}(q_3) \mathcal{N} \left[\tilde{J}_K^{\mu c}(q_1, q_2) \tilde{J}_L^{\nu c}(q_4, q_5) \right], \quad (156)$$

where K , and L depend on I in a way tabulated in Table II. In other words, for different I only the labels q and g that label form factors, RGPEP function B , and the currents are different.

The integrand can develop a singularity whenever $q_3^+ = 0$. One of the sources of possible singularities is the following expression:

$$\frac{f_{t,1245}^{K.L} B_{t,123.45(-3)}^{K.L}}{q_3^+} = (f_{t,123}^K f_{t,45(-3)}^L - f_{t,1245}^{K.L}) \mathcal{F}^{K.L}, \quad (157)$$

where

$$\mathcal{F}^{K.L} = \frac{1}{2} \left(\frac{1}{m_g^2 - (q_1|_K + q_2|_K)^2} + \frac{1}{m_g^2 - (q_4|_L + q_5|_L)^2} \right), \quad (158)$$

and $q|_K = q|_{m_K}$ with $m_K = m_q = m$ for $K = q$, and $m_K = m_g$ for $K = g$. There are two cases, either $(q_1 + q_2)^2 \leq 0$ or $(q_1 + q_2)^2 \geq 4m_K^2$. The former happens in Figs. 12(a) and (b), while the latter happens in Figs. 12(c) and (d). Similarly, either $(q_4 + q_5)^2 \leq 0$, see Figs. 12(a), (b), and (d), or $(q_4 + q_5)^2 \geq 4m_L^2$, see Fig. 12(c). We assume that m_g is much smaller than the quark mass and $4m^2 > m_g^2$. Therefore, whether m_K and m_L are m or m_g , $\mathcal{F}^{K.L}$ and Eq. (157) never develops any singularity despite explicit $1/q_3^+$ factor.

Using momentum conservation and Eq. (22),

$$q_{3\mu} \tilde{J}_K^{\mu c}(q_1, q_2) = \frac{m_g^2 - (q_1|_K + q_2|_K)^2}{2q_3^+} \tilde{J}_K^{+c}(q_1, q_2), \quad (159)$$

$$q_{3\nu} \tilde{J}_L^{\nu c}(q_4, q_5) = \frac{m_g^2 - (q_4|_L + q_5|_L)^2}{2q_3^+} \tilde{J}_L^{+c}(q_4, q_5). \quad (160)$$

Therefore, using Eq. (96),

$$d_{\mu\nu}(q_3)\mathcal{N}\left[\tilde{J}_K^{\mu c}(q_1, q_2)\tilde{J}_L^{\nu c}(q_4, q_5)\right] = -g_{\mu\nu}\mathcal{N}\left[\tilde{J}_K^{\mu c}(q_1, q_2)\tilde{J}_L^{\nu c}(q_4, q_5)\right] \\ - \frac{(q_1|_K + q_2|_K)^2 + (q_4|_L + q_5|_L)^2}{2(q_3^+)^2}\mathcal{N}\left[\tilde{J}_K^{+c}(q_1, q_2)\tilde{J}_L^{+c}(q_4, q_5)\right]. \quad (161)$$

Next, we split $\mathcal{H}_{t,2}^{(I)}$ into two terms:

$$\mathcal{H}_{t,2}^{(I)} = \mathcal{H}_{t,2}^{(I,R)} + \mathcal{H}_{t,2}^{(I,X)}, \quad (162)$$

where $\mathcal{H}_{t,2}^{(I,R)}$ is regular, while $\mathcal{H}_{t,2}^{(I,X)}$ is singular:

$$\mathcal{H}_{t,2}^{(I,R)} = -\frac{S_I}{2}\int[q_1q_2q_3q_4q_5]\tilde{\delta}_{123}\tilde{\delta}_{45,3}f_{t_r,123}^K f_{t_r,45(-3)}^L \frac{f_{t,1245}^{K,L}B_{t,123,45(-3)}^{K,L}}{q_3^+} \\ \times g_{\mu\nu}\mathcal{N}\left[\tilde{J}_K^{\mu c}(q_1, q_2)\tilde{J}_L^{\nu c}(q_4, q_5)\right] \\ - \frac{S_I}{2}\int[q_1q_2q_3q_4q_5]\tilde{\delta}_{123}\tilde{\delta}_{45,3}f_{t+t_r,123}^K f_{t+t_r,45(-3)}^L \frac{\tilde{\mathcal{F}}^{K,L}}{(q_3^+)^2} \\ \times \mathcal{N}\left[\tilde{J}_K^{+c}(q_1, q_2)\tilde{J}_L^{+c}(q_4, q_5)\right], \quad (163)$$

$$\mathcal{H}_{t,2}^{(I,X)} = \frac{S_I}{2}\int[q_1q_2q_3q_4q_5]\tilde{\delta}_{123}\tilde{\delta}_{45,3}f_{t_r,123}^K f_{t_r,45(-3)}^L f_{t,1245}^{K,L} \frac{\tilde{\mathcal{F}}^{K,L}}{(q_3^+)^2} \\ \times \mathcal{N}\left[\tilde{J}_K^{+c}(q_1, q_2)\tilde{J}_L^{+c}(q_4, q_5)\right]. \quad (164)$$

where

$$\tilde{\mathcal{F}}^{K,L} = \frac{(q_1|_K + q_2|_K)^2 + (q_4|_L + q_5|_L)^2}{2}\mathcal{F}^{K,L}. \quad (165)$$

The first term of $\mathcal{H}_{t,2}^{(I,R)}$ is not singular because it does not contain any $1/q_3^+$ factors other than those discussed in Eq. (157). The second term of $\mathcal{H}_{t,2}^{(I,R)}$ is not singular because it contains the product of form factors, $f_{t,123}^K f_{t,45(-3)}^L$. Note that

$$f_{t,123}^K f_{t,45(-3)}^L = \exp\left(-t\frac{[(q_1|_K + q_2|_K)^2 - m_g^2]^2}{(q_3^+)^2}\right)\exp\left(-t\frac{[(q_4|_L + q_5|_L)^2 - m_g^2]^2}{(q_3^+)^2}\right). \quad (166)$$

From previous analysis we know that $[(q_1 + q_2)^2 - m_g^2]^2 \geq m_g^4$ and $[(q_4 + q_5)^2 - m_g^2]^2 \geq m_g^4$, because either $(q_1 + q_2)^2 \leq 0$ or $(q_1 + q_2)^2 \geq 4m_K^2 > m_g^2$, and the analogous holds for $(q_4 + q_5)^2$. Therefore, as q_3^+ approaches zero, $f_{t,123}^K f_{t,45(-3)}^L$ approaches zero at least as quickly as $\exp[-tm_g^4(q_3^+)^{-2}]$ and can regulate any power of $1/q_3^+$. However, this conclusion changes in the $m_g \rightarrow 0$ limit, as discussed in Sec. VI.

In contrast, $\mathcal{H}_{t,2}^{(I,X)}$ contains a singular factor of $1/(q_3^+)^2$ which is regulated only by $f_{t_r,123}^K f_{t_r,45(-3)}^L$. Therefore, the matrix elements of $\mathcal{H}_{t,2}^{(I,X)}$ diverge as $t_r \rightarrow 0$. Another singular term in the effective Hamiltonian arises from the instantaneous gluon term in the canonical Hamiltonian. We define $\mathcal{H}_{t,2}^{(0,JJ)} = e^{-t(i\partial_f^-)^2} H_{JJ}$. For $I \in \{a, j, k, l\}$, $\mathcal{H}_{t,2}^{(0,JJ)} = \sum_I \mathcal{H}_{t,2}^{(0,I)}$, where

$$\mathcal{H}_{t,2}^{(0,I)} = \frac{S_I}{2} \int [q_1 q_2 q_3 q_4 q_5] \tilde{\delta}_{123} \tilde{\delta}_{45.3} f_{t_r,123}^K f_{t_r,45(-3)}^L \frac{f_{t,1245}^{K,L}}{(q_3^+)^2} \mathcal{N} \left[\tilde{J}_K^{+c}(q_1, q_2) \tilde{J}_L^{+c}(q_4, q_5) \right]. \quad (167)$$

Therefore,

$$\begin{aligned} \mathcal{H}_{t,2}^{(0,I)} + \mathcal{H}_{t,2}^{(I,X)} &= \frac{S_I}{2} \int [q_1 q_2 q_3 q_4 q_5] \tilde{\delta}_{123} \tilde{\delta}_{45.3} f_{t_r,123}^K f_{t_r,45(-3)}^L f_{t,1245}^{K,L} \\ &\quad \times \frac{1 + \tilde{\mathcal{F}}^{K,L}}{(q_3^+)^2} \mathcal{N} \left[\tilde{J}_K^{+c}(q_1, q_2) \tilde{J}_L^{+c}(q_4, q_5) \right]. \end{aligned} \quad (168)$$

We now determine the counterterm necessary to make the matrix elements of these Hamiltonian terms finite as $t_r \rightarrow 0$. Among diagrams in Fig. 12, only 12(a) and 12(b) need to be studied. This is because $q_3^+ = 0$ implies both $q_1^+ + q_2^+ = 0$ and $q_4^+ + q_5^+ = 0$. If the sign of q_1^+ is the same as the sign of q_2^+ , as in diagrams with pair creation, then q_1^+ and q_2^+ need to vanish as $q_3^+ \rightarrow 0$. Similarly, if $q_4^+ q_5^+ < 0$, as in diagrams with pair annihilation, then both $q_4^+ \rightarrow 0$ and $q_5^+ \rightarrow 0$ as $q_3^+ \rightarrow 0$. Since wave functions are compactly supported, the matrix elements cannot receive divergent contributions from diagrams with pair creation or annihilation. In diagrams 12(a) and 12(b) q_1^+ has an opposite sign to the sign of q_2^+ and q_4^+ has an opposite sign to the sign of q_5^+ . Therefore, all four momenta can remain nonzero as $q_3^+ \rightarrow 0$. Moreover, $q_1^-, q_2^-, q_4^-,$ and q_5^- are all finite. Therefore,

$$(q_1 + q_2)^2 = (q_1^+ + q_2^+)(q_1^- + q_2^-) - (q_1^\perp + q_2^\perp)^2 = -(q_3^\perp)^2, \quad (q_3^+ = 0) \quad (169)$$

$$(q_4 + q_5)^2 = (q_4^+ + q_5^+)(q_4^- + q_5^-) - (q_4^\perp + q_5^\perp)^2 = -(q_3^\perp)^2, \quad (q_3^+ = 0) \quad (170)$$

which leads to

$$\tilde{\mathcal{F}}^{K,L} = -\frac{(q_3^\perp)^2}{m_g^2 + (q_3^\perp)^2} \cdot (q_3^+ = 0) \quad (171)$$

The regulating factors are

$$f_{t_r,123}^K f_{t_r,45(-3)}^L = \exp \left[-2t_r \frac{[(q_3^\perp)^2 + m_g^2]^2}{(q_3^+)^2} + O\left(\frac{1}{q_3^+}\right) \right]. \quad (q_3^+ \rightarrow 0) \quad (172)$$

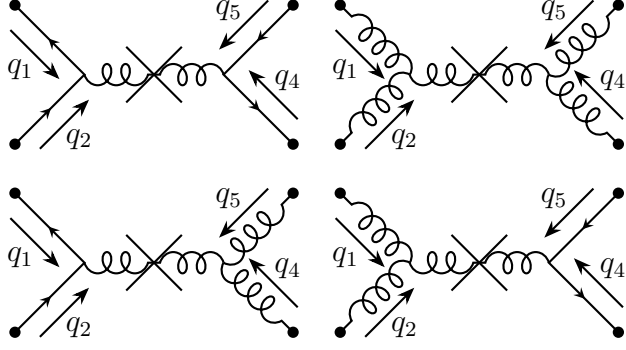


FIG. 13. Wick's diagrams for the instantaneous interaction counterterms.

Therefore, the singular factor $1/(q_3^+)^2$, multiplied by $f_{t_r,123}^K f_{t_r,45(-3)}^L$, gives in the leading order,

$$\int_{-\infty}^{\infty} \frac{dq_3^+}{(q_3^+)^2} e^{-2t_r \frac{[(q_3^\perp)^2 + m_g^2]}{(q_3^+)^2}} = \frac{1}{m_g^2 + (q_3^\perp)^2} \sqrt{\frac{\pi}{2t_r}}, \quad (173)$$

which is divergent in the $t_r \rightarrow 0$ limit. To counter this divergence we define the counterterm,

$$\begin{aligned} \mathcal{H}_{t,2}^{(0,I,X)} &= -\frac{S_I}{2} \int [q_1 q_2 q_3 q_4 q_5] \tilde{\delta}_{123} \tilde{\delta}_{45,3} f_{t,1245}^{K,L} \frac{m_g^2}{[m_g^2 + (q_3^\perp)^2]^2} \sqrt{\frac{\pi}{2t_r}} \delta(q_3^+) \\ &\times \mathcal{N} \left[\tilde{J}_K^{+c}(q_1, q_2) \tilde{J}_L^{+c}(q_4, q_5) \right]. \end{aligned} \quad (174)$$

To be more precise, the counterterm is $\mathcal{H}_{0,2}^{(0,I,X)}$ and it is added to the initial condition at $t = 0$, while $\mathcal{H}_{t,2}^{(0,I,X)}$ is the term at $t > 0$ that is produced by the RGPEP flow in the second order due to the presence of the counterterm. This counterterm extends the one introduced in Ref. [49] to all Fock sectors and all combinations of quarks, antiquarks, and gluons.

The instantaneous fermion diagrams are analyzed next. The diagrams D_b and D_c , Fig. 4 give,

$$\begin{aligned} \mathcal{H}_{t,2}^{(b)} + \mathcal{H}_{t,2}^{(c)} &= g^2 \int [q_1 q_2 q_3 q_4 q_5 q_6] \tilde{\delta}_{123} \tilde{\delta}_{56,2} f_{t_r,123}^q f_{t_r,(-2)56}^q f_{t,1356}^{q,q} \frac{B_{t,123,(-2)56}^{q,q}}{q_2^+} \\ &\times \mathcal{N} \left[\bar{\Psi}(-q_1) \gamma_\mu T^a G^{\mu a}(q_3) (\not{q}_2 + m) \gamma_\nu T^b G^{\nu b}(q_6) \Psi(q_5) \right]. \end{aligned} \quad (175)$$

The diagram, Fig. 2(a) gives,

$$\begin{aligned} \mathcal{H}_{t,2}^{(0,bc)} &= g^2 \int [q_1 q_2 q_3 q_4 q_5 q_6] \tilde{\delta}_{123} \tilde{\delta}_{56,2} f_{t_r,123}^q f_{t_r,(-2)56}^q f_{t,1356}^{q,q} \\ &\times \mathcal{N} \left[\bar{\Psi}(-q_1) \gamma_\mu T^a G^{\mu a}(q_3) \frac{\gamma^+}{2q_2^+} \gamma_\nu T^b G^{\nu b}(q_6) \Psi(q_5) \right]. \end{aligned} \quad (176)$$

The three diagrams together:

$$\begin{aligned}
\mathcal{H}_{t,2}^{(\Psi^2 G^2)} &= \mathcal{H}_{t,2}^{(b)} + \mathcal{H}_{t,2}^{(c)} + \mathcal{H}_{t,2}^{(0,bc)} \\
&= g^2 \int [q_1 q_2 q_3 q_5 q_6] \tilde{\delta}_{123} \tilde{\delta}_{56.2} f_{t_r,123}^q f_{t_r,(-2)56}^q f_{t,1356}^{q,q} \\
&\quad \times \mathcal{N} \left\{ \bar{\Psi}(-q_1) \gamma_\mu T^a G^{\mu a}(q_3) \left[A \frac{\gamma^+}{2} + \frac{B_{t,123,(-2)56}^{q,q}}{q_2^+} \left(\frac{1}{2} q_2^+ \gamma^- - q_2^\perp \gamma^\perp + m \right) \right] \right. \\
&\quad \left. \times \gamma_\nu T^b G^{\nu b}(q_6) \Psi(q_5) \right\},
\end{aligned} \tag{177}$$

$$\tag{178}$$

where

$$\begin{aligned}
A &= \frac{1}{q_2^+} + \frac{B_{t,123,(-2)56}^{q,q}}{q_2^+} \frac{m^2 + (q_2^\perp)^2}{q_2^+} \\
&= \frac{1}{2} \left(\frac{-q_1^- - q_3^-}{(q_1 + q_3)^2 - m^2} + \frac{q_5^- + q_6^-}{(q_5 + q_6)^2 - m^2} \right) \\
&\quad - \left(\frac{1}{(q_1 + q_3)^2 - m^2} + \frac{1}{(q_5 + q_6)^2 - m^2} \right) \frac{f_{t,123}^q f_{t,(-2)56}^q}{f_{t,1356}^{q,q}} \frac{m^2 + (q_2^\perp)^2}{2q_2^+}.
\end{aligned} \tag{179}$$

$$\tag{180}$$

The only difference between this expression and the expression Eq. (127) in [51] for Yukawa theory is that now we have gluons instead of scalar fields. Gluonic fields introduce some extra momentum dependence:

$$\gamma_\mu G^{\mu a}(q_3) = \frac{1}{2} \gamma^+ G^{-a}(q_3) - \gamma^j G^{ja}(q_3) = \left(\frac{q_3^j}{q_3^+} \gamma^+ - \gamma^j \right) G^{ja}(q_3). \tag{181}$$

This expression is singular only for $q_3^+ \rightarrow 0$, which in this case corresponds to the external leg and is regulated by compactness of the support of wave functions. No new $q_2^+ = 0$ singularity is introduced. Hence, the analysis proceeds as in [51] for Yukawa theory. The expression

$$\frac{B_{t,123,(-2)56}^{q,q}}{q_2^+} = \frac{1}{2} \left(\frac{1}{(q_1 + q_3)^2 - m^2} + \frac{1}{(q_5 + q_6)^2 - m^2} \right) \left(1 - \frac{f_{t,123}^q f_{t,(-2)56}^q}{f_{t,1356}^{q,q}} \right) \tag{182}$$

does not contain singularities if the sign of q_1^+ is the same as the sign of q_3^+ , i.e., $q_1^+ q_3^+ > 0$, and the sign of q_5^+ is the same as the sign of q_6^+ , i.e., $q_5^+ q_6^+ > 0$, because $(q_1 + q_3)^2 \geq (m + m_g)^2 > m^2$, and $(q_5 + q_6)^2 \geq (m + m_g)^2 > m^2$ in this case.

If $q_1^+ q_3^+ < 0$, then $(q_1 + q_3)^2 - m^2$ can become zero, but at the same time $1 - f_{t,123}^q f_{t,(-2)56}^q / f_{t,1356}^{q,q}$ becomes zero as well and regulates the expression, provided that $q_2^+ \neq 0$. However, $q_2^+ = 0$ implies $(q_1 + q_3)^2 = -(q_2^\perp)^2$, making $(q_1 + q_3)^2 - m^2$ nonzero. Therefore,

q_2^+ has to be nonzero when $(q_1 + q_3)^2 - m^2$ is zero, and the expression is indeed not singular. Analogous argument applies to the $q_5^+ q_6^+ < 0$ case as well.

We have established that vanishing of $(q_1 + q_3)^2 - m^2$ or $(q_5 + q_6)^2 - m^2$ as in Eq. (182) does not lead to divergent matrix elements. The only possible source of divergence left is when $q_2^+ \rightarrow 0$ in A in the second line of Eq. (180). This expression is also regular because $f_{t,123}^q f_{t,(-2)56}^q$ has the form $\exp[-(\text{positive number})/(q_2^+)^2]$, which makes the expression go to zero as $q_2^+ \rightarrow 0$. Therefore, no counterterm is needed for the fermion exchange diagrams.

VI. CASIMIR OPERATOR

Having taken the $t_r \rightarrow 0$ limit in Sec. V we now take the limit $m_g \rightarrow 0$. Our analysis involves the quadratic Casimir operator of $SU(3)$, which we define in terms of creation and annihilation operators. These Casimir operators were previously used by one of us in the analysis of states of tetraquarks [54]. The quadratic Casimir operator is

$$\hat{C}_2 = \hat{T}^a \hat{T}^a , \quad (183)$$

where the sum over eight colors, $a = 1, \dots, 8$, is implicit and

$$\begin{aligned} \hat{T}^a &= \sum_{\sigma, c_1, c_2} \int \frac{dp^+ d^2 p^\perp}{16\pi^3 p^+} \theta(p^+) [T_F^a]_{c_1 c_2} b_{p\sigma c_1}^\dagger b_{p\sigma c_2} \\ &+ \sum_{\sigma, c_1, c_2} \int \frac{dp^+ d^2 p^\perp}{16\pi^3 p^+} \theta(p^+) [T_{\bar{F}}^a]_{c_1 c_2} d_{p\sigma c_1}^\dagger d_{p\sigma c_2} \\ &+ \sum_{\sigma, c_1, c_2} \int \frac{dp^+ d^2 p^\perp}{16\pi^3 p^+} \theta(p^+) [T_A^a]_{c_1 c_2} a_{p\sigma c_1}^\dagger a_{p\sigma c_2} , \end{aligned} \quad (184)$$

with

$$[T_F^a]_{c_1 c_2} = T_{c_1 c_2}^a , \quad (185)$$

$$[T_{\bar{F}}^a]_{c_1 c_2} = -T_{c_2 c_1}^a , \quad (186)$$

$$[T_A^a]_{c_1 c_2} = -i f^{ac_1 c_2} . \quad (187)$$

Note that $c_1, c_2 \in \{1, 2, 3\}$ in Eqs. (185) and (186), while $c_1, c_2 \in \{1, \dots, 8\}$ in Eq. (187). Subscripts F , \bar{F} , and A refer to 3, $\bar{3}$, and 8 representations, respectively. Representation 3 is a fundamental representation associated with quarks. Representation $\bar{3}$ is a fundamental representation associated with antiquarks and $\bar{3}$ is conjugate to 3. Representation 8 is the

adjoint representation and it is associated with gluons. The color charge operators annihilate the vacuum because their terms are normal ordered,

$$\hat{T}^a |0\rangle = 0 . \quad (188)$$

Moreover,

$$\left[\hat{T}^a, b_{p\sigma c}^\dagger \right] = \sum_{c'} [T_F^a]_{c'c} b_{p\sigma c'}^\dagger , \quad (189)$$

$$\left[\hat{T}^a, d_{p\sigma c}^\dagger \right] = \sum_{c'} [T_{\bar{F}}^a]_{c'c} d_{p\sigma c'}^\dagger , \quad (190)$$

$$\left[\hat{T}^a, a_{p\sigma c}^\dagger \right] = \sum_{c'} [T_A^a]_{c'c} a_{p\sigma c'}^\dagger . \quad (191)$$

Therefore,

$$\hat{C}_2 b_{p\sigma c}^\dagger |0\rangle = C_F b_{p\sigma c}^\dagger |0\rangle , \quad (192)$$

$$\hat{C}_2 d_{p\sigma c}^\dagger |0\rangle = C_F d_{p\sigma c}^\dagger |0\rangle , \quad (193)$$

$$\hat{C}_2 a_{p\sigma c}^\dagger |0\rangle = C_A a_{p\sigma c}^\dagger |0\rangle . \quad (194)$$

where (keeping in mind implicit sum over a)

$$C_F = \sum_{c'=1}^3 [T_F^a]_{cc'} [T_F^a]_{c'c} = \sum_{c'=1}^3 [T_{\bar{F}}^a]_{cc'} [T_{\bar{F}}^a]_{c'c} = \frac{N_c^2 - 1}{2N_c} , \quad (195)$$

and

$$C_A = \sum_{c'=1}^8 [T_A^a]_{cc'} [T_A^a]_{c'c} = N_c . \quad (196)$$

Additionally, $g\hat{T}^a$ can be thought of as the charge operator. In terms of the color current operators,

$$\hat{T}^a = \frac{1}{2g} \left[J_q^{+a}(0) + 3\tilde{J}_g^{+a}(0) \right] \quad (197)$$

$$= \frac{1}{2g} \int [q] \left[\tilde{J}_q^{+a}(-q, q) + 3\tilde{J}_g^{+a}(-q, q) \right] \quad (198)$$

$$= \frac{1}{2} \int [q] \mathcal{N} \left[\bar{\Psi}(q) \gamma^+ T^a \Psi(q) \right] + \frac{1}{2} \int [q] (-i f^{c_1 c_2 a}) q^+ G^{j c_1}(-q) G^{j c_2}(q) , \quad (199)$$

where we assume $\epsilon^+ = 0$.

In accordance with Wick's theorem, the Casimir operator splits into three normal-ordered terms,

$$\hat{C}_2 = \mathcal{N} \left(\hat{T}^a \hat{T}^a \right) + \int [q] \frac{C_F |q^+|}{q^+} \mathcal{N} \left[\bar{\Psi}(q) \frac{\gamma^+}{2} \Psi(q) \right] + \int [q] \theta(q^+) C_A q^+ G^{ja}(-q) G^{ja}(q) . \quad (200)$$

The first term corresponds to gluon exchange interactions between color currents, while the other two terms correspond to mass terms in the Hamiltonian. Comparison with the free part of the Hamiltonian, Eq. (29), reveals that $C_F |q^+|$ and $C_A |q^+|$ have the correct form for a correction to the quark mass m^2 , and gluon mass m_g^2 , respectively. Therefore these are the factors that we expect to arise from the self-interaction terms. We first consider gluon self-interactions, and then quark self-interactions, and finally interactions between color currents.

Gluon self interactions have three contributions: unrenormalized gluon loop, Eq. (140), unrenormalized quark loop, Eq. (114), and the gluon mass counterterm, Eq. (155). We define the renormalized gluon loop contribution, $\delta\mu_{t,g,2}^2(q_3)$ as the sum of $\delta\tilde{\mu}_{t,g,2}^2(q_3)$ and the second term in Eq. (155):

$$\delta\mu_{t,g,2}^2(q_3) = C_A g^2 \int [q_1 q_2] \frac{\theta(q_1^+) \theta(q_2^+)}{|q_1^+| |q_2^+|} \tilde{\delta}_{12,3} q_3^+ \frac{e^{-2t \frac{\mathcal{M}_{12}^2 - m_g^2}{(q_3^+)^2}}}{\mathcal{M}_{12}^2 - m_g^2} \cdot 2k^2 \frac{(1 - x_1 x_2)^2}{(x_1 x_2)^2} , \quad (201)$$

where x_1 , x_2 , and k are defined according to Eqs. (115) and (116), and

$$\mathcal{M}_{12}^2 = \frac{m_g^2 + k^2}{x_1 x_2} . \quad (202)$$

We also define the renormalized quark loop contribution, $\delta\mu_{t,q,2}^2(q_3)$ as the sum of $\delta\tilde{\mu}_{t,q,2}^2(q_3)$ and the first term in Eq. (155):

$$\delta\mu_{t,q,2}^2(q_3) = 2T_f g^2 \int [q_1 q_2] \frac{\theta(q_1^+) \theta(q_2^+)}{|q_1^+| |q_2^+|} \tilde{\delta}_{12,3} q_3^+ \frac{e^{-2t \frac{\mathcal{M}_{12}^2 - m_g^2}{(q_3^+)^2}}}{\mathcal{M}_{12}^2 - m_g^2} (\mathcal{M}_{12}^2 - 2k^2) , \quad (203)$$

where

$$\mathcal{M}_{12}^2 = \frac{m^2 + k^2}{x_1 x_2} . \quad (204)$$

$\delta\mu_{t,q,2}^2(q_3)$ is finite in the $m_g \rightarrow 0$ limit. For $m^4 t \ll (q_3^+)^2$ it takes particularly simple form,

$$\lim_{m_g \rightarrow 0} \delta\mu_{t,q,2}^2(q_3) = \frac{g^2}{16\pi^2} |q_3^+| \sqrt{\frac{\pi}{2t}} \cdot \frac{1}{3} + o(1) . \quad (m \rightarrow 0) \quad (205)$$

The gluon loop contribution on the other hand is logarithmically divergent,

$$\delta\mu_{t,g,2}^2(q_3) = C_A|q_3^+|\frac{g^2}{16\pi^2}\sqrt{\frac{\pi}{2t}}\left[\log\left(\frac{(q_3^+)^2}{8m_g^4t}\right)-\gamma-\frac{23}{6}\right]+o(1). \quad (m_g \rightarrow 0) \quad (206)$$

Renormalized quark self interaction due to quark-gluon loop is logarithmically divergent as well,

$$\delta m_{t,2}^2 = \delta\tilde{m}_{t,2}^2 + \delta m_{t,X,2}^2 = C_F|q_1^+|\frac{g^2}{16\pi^2}\sqrt{\frac{\pi}{2t}}\log\left(\frac{1}{16m_g^4}\right)+O(1). \quad (m_g \rightarrow 0) \quad (207)$$

For $m^4t \ll (q_1^+)^2$, the expression can be evaluated further,

$$\delta m_{t,2}^2 = C_F|q_1^+|\frac{g^2}{16\pi^2}\sqrt{\frac{\pi}{2t}}\left[\log\left(\frac{(q_1^+)^2}{8m_g^4t}\right)-\gamma-\frac{7}{2}\right]+o(1). \quad (m_g \rightarrow 0, m \rightarrow 0) \quad (208)$$

The gluon self-energy and quark self-energy are composed of the expected color-momentum factors, $C_A|q_3^+|$ and $C_F|q_1^+|$, respectively, times a common divergent factor $\frac{g^2}{16\pi^2}\sqrt{\frac{\pi}{2t}}\log\left(\frac{1}{m_g^4}\right)$. The same common factor is also found in the gluon exchange terms. To show it we focus on the second term of $\mathcal{H}_{t,2}^{(I,R)}$, which contains $\tilde{J}_K^{+c}\tilde{J}_L^{+c}$, see Eq. (163). The only potential source of divergence is the vicinity of $q_3^+ = 0$. Using Eq. (171), we replace $\tilde{\mathcal{F}}^{K,L} \rightarrow -1$. The m_g term in the denominator of Eq. (171) can be neglected, because it leads to small corrections as $m_g \rightarrow 0$. Using Eq. (172), $f_{t,123}^K f_{t,45(-3)}^L$ is replaced with its approximation valid at $q_3^+ = 0$. Nonzero m_g needs to be kept here, because it regulates the logarithmic divergence. After these simplifications we arrive at

$$J^{(I)} = \frac{S_I}{2} \int [q_1 q_2 q_3 q_4 q_5] \theta(-q_1^+ q_2^+) \theta(-q_4^+ q_5^+) \tilde{\delta}_{123} \tilde{\delta}_{45,3} \exp\left(-2t \frac{[m_g^2 + (q_3^+)^2]^2}{(q_3^+)^2}\right) \times \frac{1}{(q_3^+)^2} \mathcal{N} \left[\tilde{J}_K^{+c}(q_1, q_2) \tilde{J}_L^{+c}(q_4, q_5) \right], \quad (209)$$

where one more modification to the discussed term of $\mathcal{H}_{t,2}^{(I,R)}$ has been made: we inserted $\theta(-q_1^+ q_2^+)$, which ensures that q_1^+ and q_2^+ have different signs, and $\theta(-q_4^+ q_5^+)$, which ensures that q_4^+ and q_5^+ have different signs. This is necessary to exclude pair creation and pair annihilation interaction terms, which are regulated by the compactness of the support of wave functions. Therefore, $J^{(I)}$ describes only gluon exchange between two color currents.

To evaluate $J^{(I)}$ further we change integration variables from q_1, q_2, q_4 , and q_5 to P_{12} ,

Q_{12} , P_{45} , and Q_{45} , where

$$P_{12}^{+,\perp} = \frac{q_2^{+,\perp} - q_1^{+,\perp}}{2}, \quad (210)$$

$$Q_{12}^{+,\perp} = q_1^{+,\perp} + q_2^{+,\perp}, \quad (211)$$

$$P_{45}^{+,\perp} = \frac{q_5^{+,\perp} - q_4^{+,\perp}}{2}, \quad (212)$$

$$Q_{45}^{+,\perp} = q_4^{+,\perp} + q_5^{+,\perp}. \quad (213)$$

We can easily evaluate integration over Q_{45} , and Q_{12} , because momentum conservation forces $Q_{45} = -Q_{12} = q_3$. The two theta functions become $\theta[(P_{12}^+)^2 - (q_3^+)^2/4]$, and $\theta[(P_{45}^+)^2 - (q_3^+)^2/4]$ and can be replaced with one that produces the same result: $\theta(P^+ - |q_3^+|)$, where $P^+ = 2 \min(|P_{12}^+|, |P_{45}^+|) = \min(|q_2^+ - q_1^+|, |q_5^+ - q_4^+|)$. Therefore,

$$\begin{aligned} J^{(I)} &= \frac{S_I}{2} \int [P_{12} P_{45}] \int [q_3] \theta(P^+ - |q_3^+|) \exp\left(-2t \frac{[m_g^2 + (q_3^+)^2]^2}{(q_3^+)^2}\right) \frac{1}{(q_3^+)^2} \\ &\quad \times \mathcal{N} \left[\tilde{J}_K^{+c} \left(-\frac{q_3}{2} - P_{12}, -\frac{q_3}{2} + P_{12}\right) \tilde{J}_L^{+c} \left(\frac{q_3}{2} - P_{45}, \frac{q_3}{2} + P_{45}\right) \right]. \end{aligned} \quad (214)$$

The divergence is due to the behavior of the integrand at $q_3^+ = 0$, $q_3^\perp = 0$, as $m_g \rightarrow 0$. To extract it we Taylor expand $\tilde{J}_K^{+c} \tilde{J}_L^{+c}$ in q_3 . Only the first term,

$$\begin{aligned} J_{\text{div}}^{(I)} &= \frac{S_I}{2} \int [P_{12} P_{45}] \int [q_3] \theta(P^+ - |q_3^+|) \exp\left(-2t \frac{[(q_3^\perp)^2 + m_g^2]^2}{(q_3^+)^2}\right) \frac{1}{(q_3^+)^2} \\ &\quad \times \mathcal{N} \left[\tilde{J}_K^{+c}(-P_{12}, P_{12}) \tilde{J}_L^{+c}(-P_{45}, P_{45}) \right] \end{aligned} \quad (215)$$

is divergent. Integration over q_3 gives

$$\begin{aligned} &\int [q_3] \theta(P^+ - |q_3^+|) \exp\left(-2t \frac{[(q_3^\perp)^2 + m_g^2]^2}{(q_3^+)^2}\right) \frac{1}{(q_3^+)^2} \\ &= \frac{1}{2} \frac{1}{16\pi^2} \sqrt{\frac{\pi}{2t}} \left[\log\left(\frac{(P^+)^2}{8m_g^4 t}\right) - \gamma \right] + O(m_g^2). \end{aligned} \quad (216)$$

Note that the above result depends on P_{12}^+ and P_{45}^+ through P^+ . To obtain \hat{T}^a in Eq. (215) we need to work around this dependence, because Eq. (198) does not contain any $\log|q^+|$ factors. Fortunately we can replace P^+ with some \mathcal{P}^+ that does not depend on neither P_{12}^+ or P_{45}^+ , because $\log[(P^+)/m_g^4] = \log[(\mathcal{P}^+)/m_g^4] + \log(P^+/\mathcal{P}^+)$ and $\log(P^+/\mathcal{P}^+)$ is $O(1)$ as $m_g \rightarrow 0$. Therefore,

$$J_{\text{div}}^{(I)} = \frac{g^2}{16\pi^2} \sqrt{\frac{\pi}{2t}} \log\left(\frac{(\mathcal{P}^+)^2}{8m_g^4 t}\right) \mathcal{N}(\hat{T}_K^c \hat{T}_L^c) + O(1), \quad (m_g \rightarrow 0) \quad (217)$$

where

$$\hat{T}_q^a = \frac{1}{2g} \int [q] \tilde{J}_q^{+a}(-q, q) , \quad (218)$$

$$\hat{T}_g^a = \frac{3}{2g} \int [q] \tilde{J}_g^{+a}(-q, q) . \quad (219)$$

Note that the appropriate factors of 3 for \hat{T}_g^a come from the symmetry factor, S_I . Summing $\hat{T}_K^c \hat{T}_L^c$ over all four values of $I \in \{a, j, k, l\}$ gives $\hat{T}^c \hat{T}^c$.

To recover all three terms of Eq. (200) with a common diverging factor we replace logarithms of momenta in Eqs. (206) and (208) with $\log \mathcal{P}^+$. Therefore, the effective Hamiltonian is,

$$\mathcal{H}_{t,2} = \frac{g^2}{16\pi^2} \sqrt{\frac{\pi}{2t}} \left[\log \left(\frac{(\mathcal{P}^+)^2}{8m_g^4 t} \right) - \gamma \right] \hat{T}^c \hat{T}^c + O(1) . \quad (m_g \rightarrow 0) \quad (220)$$

We see from Eq. (220) that the logarithmically divergent term in the effective Hamiltonian as $m_g \rightarrow 0$ is proportional to the Casimir operator, Eq. (183). As a consequence the divergent term vanishes in the color singlet sector, which is the eigenvalue zero eigenspace of the Casimir operator. This result generalizes the cancellation of infrared divergences observed in the quark-antiquark sector in Ref. [49]. The same kind of cancellation has been pointed out in Ref. [37], but to our knowledge no Casimir operator has been previously reported.

It is worth pointing out that even though matrix elements of $\mathcal{H}_{t,2}$ are logarithmically divergent between states that are not color singlets, color nonsinglet quantities that are produced from these matrix elements might still be well-defined. For example, single-quark mass eigenvalue is well-defined in the $m_g \rightarrow 0$ limit as long as it is computed using bound state perturbation theory up to second order with m taken as the unperturbed mass. To obtain the mass eigenvalue one has to add the second-order mass term from $\mathcal{H}_{t,2}$ and the product of two first-order vertices, as per bound state perturbation theory. The summation leads to the cancellation of m_g -divergent terms [49]. Nonperturbatively, this cancellation may be incomplete, which would lead to divergent quark eigenmass. Such lack of cancellation would simply mean that the perturbation theory with m as the unperturbed eigenmass is not the proper setup. In Ref. [49] the obstruction to the cancellation is provided by the gluon mass ansatz.

The same gluon exchange Hamiltonian term that contributes to the Casimir operator also provides a logarithmic confining potential at large separations [37, 49]. It is very satisfying that confinement removes the divergences associated with vanishing gluon mass. The

alternative would be the introduction of counter terms arising from finite gluon mass. One would expect that the finite part of such counter terms may cause the effective Hamiltonian to deviate from QCD, and so the absence of such counter terms is a positive feature of this effective Hamiltonian. We have only shown that this is true to second order in the solution of the RGPEP equations. It is an interesting question whether this is a general feature of gluon mass regularization on the light-front, i.e. whether the divergent mass terms are proportional to Casimir operators, or functions thereof, at all orders in RGPEP.

VII. SUMMARY OF THE EFFECTIVE HAMILTONIAN

The mass terms of the effective Hamiltonian are:

$$\begin{aligned} \mathcal{H}_{\text{mass}} = & \int [q] \frac{m_t^2(q) + (q^\perp)^2}{q^+} \mathcal{N} \left[\bar{\Psi}(q) \frac{\gamma^+}{2} \Psi(q) \right] \\ & + \int [q] \theta(q^+) \frac{\mu_t^2(q) + (q^\perp)^2}{q^+} \mathcal{N} [G^{ia}(-q) G^{ia}(q)], \end{aligned} \quad (221)$$

where

$$\begin{aligned} m_t^2(q) = & m^2 + C_F g^2 \int [q_2 q_3] \tilde{\delta}_{23,q} \frac{\theta(q_2^+) \theta(q_3^+)}{q_2^+ q_3^+} \frac{(f_{t,(-q)23}^q)^2}{q_2^-|_m + q_3^-|_{m_g} - q_1^-|_m} \\ & \times d_{\mu\nu}(q_3) \bar{u}_\sigma(q) \gamma^\mu (q_2 + m) \gamma^\nu u_\sigma(q) + \delta m_{\text{finite},2}^2. \end{aligned} \quad (222)$$

$$\begin{aligned} \mu_t^2(q) = & m_g^2 + 2T_f g^2 \int [q_1 q_2] \frac{\theta(q_1^+) \theta(q_2^+)}{q_1^+ q_2^+} \tilde{\delta}_{12,q} \frac{(f_{t,12(-q)}^q)^2}{q_1^-|_m + q_2^-|_m - q^-|_{m_g}} [\mathcal{M}_{12}^2 - 2(k^\perp)^2] \\ & + C_A g^2 \int [q_1 q_2] \frac{\theta(q_1^+) \theta(q_2^+)}{q_1^+ q_2^+} \tilde{\delta}_{12,q} \frac{(f_{t,12(-q)}^g)^2}{q_1^-|_{m_g} + q_2^-|_{m_g} - q^-|_{m_g}} 2(k^\perp)^2 \frac{(1 - x_1 x_2)^2}{(x_1 x_2)^2} \\ & + \delta \mu_{\text{finite},2}^2. \end{aligned} \quad (223)$$

In our previous analysis of RGPEP for the Yukawa model [51] we fixed the analogous finite part of the fermion counterterm by demanding the physical mass of the fermion to be equal to the unperturbed mass in the Hamiltonian. In the second order of perturbation theory the physical mass receives contributions from the second-order self-energy terms in the Hamiltonian, such as those in Eq. (104), and from a product of two first-order vertices arising from bound state perturbation theory. Our condition forces these two contributions to cancel exactly. If we were to use the same condition here, then $\delta m_{\text{finite},2}^2 = \delta \mu_{\text{finite},2}^2 = 0$. Strictly speaking, we cannot use the same argument because a single free quark and a

single free gluon are forbidden by color confinement. However, this is the unique choice which ensures $m_t^2(q) \rightarrow m^2$, and $\mu_t^2(q) \rightarrow m_g^2$, as $t \rightarrow \infty$, which is consistent with coupling coherence, see discussion below Eq. (143) in Ref. [42]. For the time being we leave the finite parts of the mass counterterms unspecified.

The first order vertices give rise to terms:

$$\begin{aligned} \mathcal{H}_{t,1} &= g \int [q_1 q_2 q_3] \tilde{\delta}_{123} f_{t,123}^q \mathcal{N} \left[\bar{\Psi}(-q_1) \gamma_\mu T^a \Psi(q_2) G^{\mu a}(q_3) \right] \\ &+ \frac{g}{3!} \int [q_1 q_2 q_3] \tilde{\delta}_{123} f_{t,123}^g F_{\alpha\beta\gamma}^{abc}(q_1, q_2, q_3) G^{\alpha a}(q_1) G^{\beta b}(q_2) G^{\gamma c}(q_3). \end{aligned} \quad (224)$$

The second order vertices give rise to terms:

$$\mathcal{H}_{t,2}^{(G^4)} = \frac{g^2}{4!} \int [q_1 q_2 q_3 q_4] f_{t,1234} \tilde{\delta}_{1234} F_{\alpha\beta\gamma\delta}^{abcd} \mathcal{N} \left[G^{\alpha a}(q_1) G^{\beta b}(q_2) G^{\gamma c}(q_3) G^{\delta d}(q_4) \right], \quad (225)$$

The Hamiltonian includes current-current interactions:

$$\mathcal{H}_{t,2}^{(KL)} = \mathcal{H}_{t,2}^{(I,R)} + \mathcal{H}_{t,2}^{(0,I)} + \mathcal{H}_{t,2}^{(I,X)} + \mathcal{H}_{t,2}^{(0,I,X)}, \quad (226)$$

where

$$\begin{aligned} \mathcal{H}_{t,2}^{(I,R)} &= -\frac{S_I}{2} \int [q_1 q_2 q_3 q_4 q_5] \tilde{\delta}_{123} \tilde{\delta}_{45.3} \frac{f_{t,1245}^{K.L} B_{t,123.45(-3)}^{K.L}}{q_3^+} g_{\mu\nu} \mathcal{N} \left[\tilde{J}_K^{\mu c}(q_1, q_2) \tilde{J}_L^{\nu c}(q_4, q_5) \right] \\ &- \frac{S_I}{2} \int [q_1 q_2 q_3 q_4 q_5] \tilde{\delta}_{123} \tilde{\delta}_{45.3} f_{t,123}^K f_{t,45(-3)}^L \frac{\tilde{\mathcal{F}}^{K.L}}{(q_3^+)^2} \mathcal{N} \left[\tilde{J}_K^{+c}(q_1, q_2) \tilde{J}_L^{+c}(q_4, q_5) \right], \end{aligned} \quad (227)$$

and

$$\begin{aligned} \mathcal{H}_{t,2}^{(0,I)} + \mathcal{H}_{t,2}^{(I,X)} &= \frac{S_I}{2} \int [q_1 q_2 q_3 q_4 q_5] \tilde{\delta}_{123} \tilde{\delta}_{45.3} f_{t,r,123}^K f_{t,r,45(-3)}^L f_{t,1245}^{K.L} \\ &\times \frac{1 + \tilde{\mathcal{F}}^{K.L}}{(q_3^+)^2} \mathcal{N} \left[\tilde{J}_K^{+c}(q_1, q_2) \tilde{J}_L^{+c}(q_4, q_5) \right], \quad (228) \\ \mathcal{H}_{t,2}^{(0,I,X)} &= -\frac{S_I}{2} \int [q_1 q_2 q_3 q_4 q_5] \tilde{\delta}_{123} \tilde{\delta}_{45.3} f_{t,1245}^{K.L} \frac{m_g^2}{[m_g^2 + (q_3^\perp)^2]^2} \sqrt{\frac{\pi}{2t_r}} \delta(q_3^+) \\ &\times \mathcal{N} \left[\tilde{J}_K^{+c}(q_1, q_2) \tilde{J}_L^{+c}(q_4, q_5) \right]. \end{aligned} \quad (229)$$

The final term in the effective Hamiltonian is a seagull term of the following form:

$$\begin{aligned} \mathcal{H}_{t,2}^{(\Psi^2 G^2)} &= g^2 \int [q_1 q_2 q_3 q_5 q_6] \tilde{\delta}_{123} \tilde{\delta}_{56.2} f_{t,1356}^{q,q} \\ &\times \mathcal{N} \left\{ \bar{\Psi}(-q_1) \gamma_\mu T^a G^{\mu a}(q_3) \left[\frac{\gamma^+}{2q_2^+} + \frac{B_{t,123(-2)56}^{q,q}}{q_2^+} (\not{q}_2 + m) \right] \gamma_\nu T^b G^{\nu b}(q_6) \Psi(q_5) \right\}. \end{aligned} \quad (230)$$

This second order RGPEP Hamiltonian for light-front QCD is rather compact. In section VIII we will discuss some of the properties of this Hamiltonian.

VIII. CONCLUSION

In this work we have derived the second order RGPEP Hamiltonian for light-front QCD. The resulting Hamiltonian has many interesting features. Once ultraviolet renormalization is performed no new infrared divergences due to the finite gluon mass as a regulator are found. This is because the divergent terms involving the gluon mass are proportional to the quadratic Casimir operator of $SU(3)$ and hence vanish in the color singlet sector of physical states. The Hamiltonian includes a logarithmic confining potential, which has previously reported by Perry in [37] and by Serafin [49]. The Hamiltonian is relatively compact, which is promising from the point of view future numerical work and of resource estimates for quantum computation of the kind previously carried out for the RGPEP Yukawa Hamiltonian in [55].

Naturally the physical validity of this RGPEP Hamiltonian can only be established through further analytic and computational work. A natural theoretical question is whether \mathcal{H}_t lead to perturbation theory that is the same as the standard perturbative QCD? Whether the RGPEP Hamiltonian at second order is sufficient to capture the full physics of QCD, including confinement and chiral symmetry breaking remains to be seen.

The development of this Hamiltonian made further use of the Wick diagram techniques introduced previously in [51]. We hope that these techniques will enable RGPEP calculations to higher order if we find that the second order Hamiltonian does not contain all the physics of QCD. Finally, we hope that this and future work will shed further light on questions of renormalizability on the light-front.

-
- [1] S. J. Brodsky, H.-C. Pauli, and S. S. Pinsky, Phys. Rept. **301**, 299 (1998), arXiv:hep-ph/9705477.
 - [2] B. L. G. Bakker et al., Nucl. Phys. B Proc. Suppl. **251-252**, 165 (2014), arXiv:1309.6333 [hep-ph].
 - [3] S. D. Glazek, Nucl. Phys. B Proc. Suppl. **90**, 175 (2000).
 - [4] S. D. Glazek, Acta Phys. Polon. B **43**, 1843 (2012), arXiv:1204.4760 [hep-th].
 - [5] S. P. Jordan, K. S. M. Lee, and J. Preskill, Science **336**, 1130 (2012), arXiv:1111.3633 [quant-ph].

- [6] S. P. Jordan, K. S. M. Lee, and J. Preskill, *Quant. Inf. Comput.* **14**, 1014 (2014), arXiv:1112.4833 [hep-th].
- [7] S. P. Jordan, K. S. M. Lee, and J. Preskill, (2014), arXiv:1404.7115 [hep-th].
- [8] T. Maslowski and M. Wieckowski, *Phys. Rev. D* **57**, 4976 (1998), arXiv:hep-th/9707057.
- [9] K. Serafin, Model of renormalization of masses and coupling constants, Master's thesis, University of Warsaw, Warsaw (2015), (in Polish).
- [10] M. Wieckowski, (2005), arXiv:hep-th/0511148.
- [11] J. Collins, (2018), arXiv:1801.03960 [hep-ph].
- [12] S.-J. Chang and S.-K. Ma, *Phys. Rev.* **180**, 1506 (1969).
- [13] P. D. Mannheim, P. Lowdon, and S. J. Brodsky, *Phys. Rept.* **891**, 1 (2021), arXiv:2005.00109 [hep-ph].
- [14] W. Polyzou, *Phys. Rev. D* **103**, 105017 (2021), arXiv:2102.05525 [hep-th].
- [15] K. Hornbostel, The Application of Light Cone Quantization to Quantum Chromodynamics in One-Plus-One Other thesis (1988).
- [16] K. Hornbostel, S. J. Brodsky, and H. C. Pauli, *Phys. Rev. D* **41**, 3814 (1990).
- [17] S. Xu, Y. Liu, C. Mondal, J. Lan, X. Zhao, Y. Li, and J. P. Vary (BLFQ), *Phys. Lett. B* **867**, 139599 (2025), arXiv:2408.11298 [hep-ph].
- [18] S. S. Chabysheva and J. R. Hiller, *Eur. Phys. J. ST* **235**, 1451 (2026), arXiv:2502.01775 [hep-th].
- [19] E. Tomboulis, *Phys. Rev. D* **8**, 2736 (1973).
- [20] A. Casher, *Phys. Rev. D* **14**, 452 (1976).
- [21] G. P. Lepage and S. J. Brodsky, *Phys. Rev. D* **22**, 2157 (1980).
- [22] W.-M. Zhang and A. Harindranath, *Phys. Rev. D* **48**, 4868 (1993), arXiv:hep-th/9302119.
- [23] W.-M. Zhang and A. Harindranath, *Phys. Rev. D* **48**, 4881 (1993).
- [24] A. Harindranath and W.-M. Zhang, *Phys. Rev. D* **48**, 4903 (1993).
- [25] R. J. Perry, A. Harindranath, and W.-M. Zhang, *Phys. Lett. B* **300**, 8 (1993).
- [26] X. Zhao, K. Fu, H. Zhao, and J. P. Vary, *PoS LC2019*, 090 (2020), arXiv:2103.06719 [hep-ph].
- [27] J. P. Vary, C. Mondal, S. Xu, X. Zhao, and Y. Li (BLFQ), *Eur. Phys. J. ST* **235**, 1557 (2026), arXiv:2512.08283 [hep-ph].
- [28] R. J. Perry, A. Harindranath, and K. G. Wilson, *Phys. Rev. Lett.* **65**, 2959 (1990).
- [29] R. J. Perry and A. Harindranath, *Phys. Rev. D* **43**, 4051 (1991).

- [30] V. A. Karmanov, J. F. Mathiot, and A. V. Smirnov, *Phys. Rev. D* **77**, 085028 (2008), arXiv:0801.4507 [hep-th].
- [31] J. R. Hiller, *Prog. Part. Nucl. Phys.* **90**, 75 (2016), arXiv:1606.08348 [hep-ph].
- [32] S. A. Paston, V. A. Franke, and E. V. Prokhvatilov, *Theor. Math. Phys.* **120**, 1164 (1999), arXiv:hep-th/0002062.
- [33] S. Dalley and G. McCartor, *Annals Phys.* **321**, 402 (2006), arXiv:hep-ph/0406287.
- [34] S. D. Glazek and K. G. Wilson, *Phys. Rev. D* **48**, 5863 (1993).
- [35] S. D. Glazek and K. G. Wilson, *Phys. Rev. D* **49**, 4214 (1994).
- [36] K. G. Wilson, T. S. Walhout, A. Harindranath, W.-M. Zhang, R. J. Perry, and S. D. Glazek, *Phys. Rev. D* **49**, 6720 (1994), arXiv:hep-th/9401153.
- [37] R. J. Perry, in 4th International Workshop on Light Cone Quantization and Non-Perturbative Dynamics (1994) arXiv:hep-th/9411037.
- [38] D. Chakrabarti and A. Harindranath, *Phys. Rev. D* **65**, 045001 (2002), arXiv:hep-th/0110156.
- [39] M. M. Brisudova and R. Perry, *Phys. Rev. D* **54**, 1831 (1996), arXiv:hep-ph/9511443.
- [40] M. M. Brisudova, R. J. Perry, and K. G. Wilson, *Phys. Rev. Lett.* **78**, 1227 (1997), arXiv:hep-ph/9607280.
- [41] R. J. Perry and K. G. Wilson, *Nucl. Phys. B* **403**, 587 (1993).
- [42] R. J. Perry, *Phys. Rept.* **348**, 33 (2001).
- [43] B. H. Allen and R. J. Perry, *Phys. Rev. D* **62**, 025005 (2000), arXiv:hep-th/9908124.
- [44] S. D. Glazek, *Phys. Rev. D* **69**, 065002 (2004), arXiv:hep-th/0307064.
- [45] S. D. Glazek and J. Mlynik, *Phys. Rev. D* **74**, 105015 (2006), arXiv:hep-th/0606235.
- [46] S. D. Głazek, M. Gómez-Rocha, J. More, and K. Serafin, *Phys. Lett. B* **773**, 172 (2017), arXiv:1705.07629 [hep-ph].
- [47] K. Serafin, M. Gómez-Rocha, J. More, and S. D. Głazek, *Eur. Phys. J. C* **78**, 964 (2018), arXiv:1805.03436 [hep-ph].
- [48] T. Masłowski, Relativistic description of gluonium using effective gluons in QCD, Phd thesis, University of Warsaw, Warsaw (2005), (in Polish).
- [49] K. Serafin, M. Gómez-Rocha, J. More, and S. D. Głazek, *Phys. Rev. D* **109**, 016017 (2024), arXiv:2310.00365 [hep-ph].
- [50] M. Gómez-Rocha and S. D. Głazek, *Phys. Rev. D* **92**, 065005 (2015), arXiv:1505.06688 [hep-ph].

- [51] K. Serafin, C. M. Gustin, and P. J. Love, Phys. Rev. D **112**, 096003 (2025), arXiv:2508.02972 [hep-ph].
- [52] M. Burkardt, Phys. Rev. D **47**, 4628 (1993).
- [53] M. Burkardt, Nucl. Phys. A **670**, 72 (2000).
- [54] Z. Kuang, K. Serafin, X. Zhao, and J. P. Vary (BLFQ), Phys. Rev. D **105**, 094028 (2022), arXiv:2201.06428 [hep-ph].
- [55] C. M. Gustin, K. Serafin, W. A. Simon, A. Ralli, G. R. Goldstein, and P. J. Love, Physical Review D **113**, 016018 (2026).